RE-CHARACTERIZATION OF NIGERIA RESEARCH REACTOR-1 IRRADIATION CHANNELS BEFORE CONVERSION FROM HEU TO LEU

BY

JAMILU ABDULLAHI YUSUF

DEPARTMENT OF PHYSICS

FACULTY OF PHYSICAL SCIENCE

AHMADU BELLO UNIVERSITY, ZARIA

NIGERIA

OCTOBER 2018

RE-CHARACTERIZATION OF NIGERIA RESEARCH REACTOR-1 IRRADIATION CHANNELS BEFORE CONVERSION FROM HEU TO LEU

BY

JAMILU ABDULLAHI YUSUF

B.TECH ENGINEERING PHYSICS (ATBU) 2011

P13SCPY8011

A DISSERTATION SUBMITTED TO THE SCHOOL OF POSTGRADUATE STUDIES, AHMADU BELLO UNIVERSITY, ZARIA NIGERIA IN PARTIAL FULFILMENT FOR THE REQUIREMENTS OF THE AWARD OF MASTERS (MSc) DEGREE IN NUCLEAR PHYSICS

DEPARTMENT OF PHYSICS
FACULTY OF PHYSICAL SCIENCE
AHMADU BELLO UNIVERSITY, ZARIA NIGERIA

OCTOBER 2018

DECLARATION

I declare that the work in this dissertation titled "RE-CHARACTERIZATION OF NIGERIA RESEARCH REACTOR-1 IRRADIATION CHANNELS BEFORE CONVERSION FROM HEU TO LEU" has been carried out by me in the Department of Physics. The information derived from the literature has been duly acknowledged in the text and a list of references provided. No part of this dissertation was previously presented for another degree at this or any other institution.

_____	_____	_____
Name	Signature	Date

CERTIFICATION

This thesis entitled RE-CHARACTERIZATION OF NIGERIA RESEARCH REACTOR-1 IRRADIATION CHANNELS BEFORE CONVERSION FROM HEU TO LEU by Jamilu Abdullahi YUSUF meets the regulations governing the award of the degree of Masters of Nuclear Physics of the Ahmadu Bello University, and is approved for its contribution to knowledge and literary presentation.

Prof. S.A Jonah	_____	_____
Chairman, Supervisory Committee	Signature	Date
Prof. U. Sadiq	_____	_____
Member, Supervisory Committee	Signature	Date
Prof. R. Nasiru	_____	_____
Head of Department	Signature	Date
Prof. S. Z. Abubakar	_____	_____
Dean, School of Postgraduate Studies	Signature	Date

DEDICATION

This work is dedicated to my family.

ACKNOWLEDGEMENT

I wish to express my sincere gratitude to Prof. S. A. Jonah and Dr. U. Sadiq for their patience, guidance and understanding throughout the course of this work.

I also wish to express my appreciation to Dr. Y.A. Ahmed, Prof. B.B.M. Dewu, Engr. I.B. Mansir, Engr. A.A.Jaoji, Mr. T. Muhammad, Engr. S. Aliyu, Engr. N.Abubakar, Engr. A.R. Abubakar, Prof. D.J. Adeyemo Mal. S. Umar, Mal. I. A. Bappah and Dr. F.T. Sheyin, Mal. M.S. Anas for their encouragement, support and prayers, and my other colleagues in the Centre for Energy Research and Training, Ahmadu Bello University Zaria, for the roles they played variously in the course of this work. I thank you all.

The prayers and support of my family was also instrumental to the completion of this work.

Finally, my sincere appreciation and gratitude also goes to all my friends.

ABSTRACT

In 2004, the first Nigerian Research Reactor (NIRR-1) was commissioned at the Centre for Energy Research and Training (CERT) Ahmadu Bello University, Zaria. NIRR-1 is a Miniature Neutron Source Reactor (MNSR) designed mainly for neutron activation analysis and personnel training. The MNSR is a compact low power reactor fueled with highly enriched uranium, cooled by natural convection and noted to possess long–term stable and reproducible neutron fluxes. Despite the stable nature of the MNSR, the neutron flux parameters in the core vary over time due to loss of reactivity from fuel burn up, accumulation of fission products and various poisons buildup in the core. Since commissioning of the reactor in 2004, a number of modifications have been effected on NIRR-1 which might have affected the neutron flux parameters in the reactor core. The spectral properties of the irradiation sites are best described by the ratio of thermal flux to epithermal flux *(f),* and the non-ideality of the epithermal neutron flux shape factor (α). Consequently, with these modifications and imminent conversion from Highly Enriched Uranium (HEU) to Low Enriched Uranium (LEU), this work was performed to determine the neutron flux parameters in an inner and an outer channels of the current HEU. The epithermal shape factor, α, and the thermal to epithermal flux ratio, *f,* were experimentally determined for two irradiation channels of NIRR-1 using Cd-ratio method with standard monitors, Al-0.1%AU, 99.5%Zn, 99.99%Zr.an high purity Zr and Zn foils of 0.125 mm thickness. The result obtained from ^{197}AU, ^{94}Zr and ^{64}Zn are: $\alpha = -0.0469$ and $f = 17.82$ for the inner irradiation channel B_2 and for the outer irradiation channel B_4 $\alpha = +0.0244$ and $f = 49.5$.The result obtained compares very well with the data measured in 2005, at the beginning of operation of the reactor, and will be used as a baseline data to develop the protocol for NAA post conversion to LEU.

TABLE OF CONTENTS

Cover Page		i
Title Page		iii
Declaration		iv
Certification		v
Dedication		vi
Acknowledgement		vii
Abstract		viii
Table of contents		ix
List of Figures		xi
List of Tables		xii
List of Plates		xiii
List of Abbreviations and Symbols		xiv
CHAPTER ONE: INTRODUCTION		1
1.1	**Background**	1
1.2	**Neutron Flux Distribution**	2
1.3	**The Epithermal Neutron Flux Spectrum**	5
1.4	**Principles of activation analysis**	6
1.5	**Aim and Objectives**	9
1.6	**Justification**	9
1.7	**Previous Work**	10
CHATER TWO: LITERATURE REVIEW		14
2.1	**Sources of Neutrons**	14
2.1.1	Nuclear Reactors	14
2.1.2	Description of NIRR-1	15
2.2	**Neutron Activation Analysis**	19
2.3	**Reaction Rate**	22
2.4	**Thermal and epithermal activation**	23
2.4.1	The epithermal reaction rate	25
2.5	The activation formula	29

2.6 **Radiation Measuring Devices** 30

2.7 **Sensitivities & Detection Limits** 31

CHAPTER THREE: **MATERIALS AND METHODS** 32

3.1 **Materials** 32

3.1.1 The irradiation facility 32

3.1.2 Pneumatic Irradiation Rabbit Transfer System (PIRS) 32

3.1.3 Gamma-ray counting equipment 33

3.1.4 Activation Foils 35

3.2 **Methodology** 37

3.2.1 Foil Irradiations 37

3.2.2 Foil counting/Gamma- ray spectrometry measurement 37

3.2.3 Determination of specific activity 38

3.2.4 Determination of the cadmium ratio 38

3.2.5 Determination of reactor neutron spectrum parameters 39

CHAPTER FOUR: RESULTAND DISCUSION 42

4.1 **Preamble** 42

4.2 **Results of neutron spectrum parameter in Channel B_2** 43

4.3 **Results of neutron spectrum parameter in Channel B_4** 46

CHAPTER FIVE: SUMMARY 51

5.1 **Conclusion** 51

5.2 **Recommendation** 52

REFERENCES 53

LIST OF FIGURES

Figure 1.1: A Schematic neutron flux spectrum of a nuclear reactor 4

Figure.2.1: Schematic longitudinal section of MNSR vessel 18

Figure 3.2: The Electronics Block Diagram of HPGe Gamma – Ray Spectrometer. 34

Figure.4.1: Excel spread sheet indicating the iteration performed to determine Reactor parameters (α, f and $Q_0(\alpha)$) for Channel B2 based on cadmium dual ratio itor momethod. 44

Figure. 4.2: Cd Ratio multi monitor method Channel B2 NIRR-1 45

Figure.4.3: Excel spread sheet indicating the iteration performed to determine reactor parameters (α, f and $Q_0(\alpha)$) for Channel B2 based on cadmium ratio dual monitor method. 46

Figure. 4.4: Cd Ratio multi monitor method Channel B4 NIRR-1 47

LIST OF TABLES

Table 2.1: Main Specifications of NIRR-1 17

Table 3.1; Characteristics of an GEM-70-S HPGe Coaxial Detector (ORTEC) 33

Table 3.2. Physical characteristics of foils used for neutron spectrum monitoring 35

Table 3.3: Nuclear data for the used foils 35

Table.4.1: Nuclear data and Cadmium ratios for Channels B_2 and B_4 42

Table.4.3: Cadmium ratios for Channels B_2 and B_4 43

Table 4.3: Summary of neutron flux parameters obtained using Cd ratio method 45

Table 4.4: f and α values for channels B_2 and B_4 of NIRR-1 determined after commissioning in 2004. 48

Table 4.5. Flux parameters obtained in this work for NIRR-1 compared with previous results obtained in NIRR-1 and data for GHARR-1 in comparison with data for the prototype MNSR and other similar facilities 50

LIST OF PLATES

Plate I: HpGE Detector Set-up 32

Plate. 2: Set of monitors irradiated in bare condition and with 1mm cadmium cover in Polystyrene vials 34

LIST OF ABBREVIATIONS AND SYMBOLS

eV	electron volts
keV	kilo electron volts
MeV	mega electron volts
NIRR-1	Nigeria Research Reactor -1
MNSR	Miniature Neutron Source Reactor
IAEA	International Atomic Energy Agency
$n/cm^2.s$	neutron per centimeter square per second
NAA	Neutron activation analysis
ENAA	epithermal neutron activation analysis
ko-NAA	single comparator method of neutron actvation analysis
Cd	cadmium
f	thermal to epithermal neutron flux ratio
φ_{th}	thermal neutron flux
φ_{epi}	epithermal neutron flux
α	epithermal neutron shape factor
σ_{th}	thermal neutron cross section
I_o	resonance integral in 1/E epithermal neutron spectrum
Q_o	resonance integral to thermal neutron cross section ration in the
1/E	epithermal neutron spectrum
$I_o(\alpha)$	resonance integral in the $1/E1+\alpha$ epithermal neutron spectrum
$Q_o(\alpha)$	resonance integral to thermal neutron cross section ration in $1/E1+\alpha$
	epithermal neutron spectrum
G_{th}	thermal neutrons self-shielding factor
G_{epi}	epithermal neutrons self-shielding factor
R_{cd}	Cadmium Ratio

CHAPTER ONE

INTRODUCTION

1.1 Background

The Nigeria Research Reactor-1 (NIRR-1) a miniature neutron source reactor (MNSR) is a compact, thermal and low power research reactor designed by the Chinese Institute of Atomic Energy mainly for purposes of neutron activation analysis (NAA), personnel training in nuclear techniques and production some short-lived radioisotope (Jonah *et al.*, 2005; SAR, 2012).The MNSR adopts tank-in-pool type structure, fueled with high-enriched uranium, and uses light water as moderator, coolant and shield. Even though MNSRs are noted to possess long – term stable and reproducible neutron fluxes, nevertheless, due to the small size of the core which aids neutron leakage, loss of reactivity from fuel burn up, accumulation of fission products and various poisons buildup, the neutron fluxes in the core reduces over time (Shokr *et al*., 2009).

The neutron flux parameters affects the reaction rate as well as the fuel burn up, thus it is a crucial parameter to know in the analysis of nuclear reactor (di Tigliole *et.al*, 2014). Moreover, a very precise knowledge of the flux in the irradiation sites is helpful for benchmarking the simulation models of the reactor. The spectral properties of the irradiation sites are best described by the ratio of thermal flux to epithermal flux *(f)*, and the epithermal neutron flux shape factor (α) (Radulović *et al.*,2014). As the MNSR is specifically designed for use in Neutron Activation Analysis (NAA), there is the need for a detailed characterization of the neutron flux parameters in the irradiation sites in order to enhance its application (Kennedy *et al.*, 2000; Akaho *et al.*, 2002; Acharya *et al.*, 2003 and Sadiq *et al.*, 20010).

1.2 Neutron Flux Distribution

The energies of neutrons produced as a result of nuclear fission spread continuously over a broad energy range up to 25 MeV and are far too energetic to efficiently promote the activation of isotopes required for conventional neutron activation analysis. Their energies are moderated by interaction with a material of low atomic number (e.g. H_2O, D_2O, graphite) in which efficient loss of kinetic energy occurs. The three types of neutrons can easily be distinguished in order of decreasing energy:

• Fast or fission neutrons. They are mainly produced by the fission of ^{235}U and still unmoderated. The most probable energies are about l MeV and predominantly promote (n, p) and (n, α) nuclear reactions. Reactions with fast neutrons are generally considered to be interferences in conventional instrumental neutron activation analysis (INAA). The fraction of fast neutrons in a thermal neutron spectrum normally used for INAA is low, but varies according to the irradiation position relative to the reactor core (Decorte, 1987, Verheijke, 1992). Since the cross section becomes smaller in the MeV region the contribution of the neutron induced (n,γ) reaction rate can be neglected.

• Epithermal, resonance or intermediate neutrons. These are the neutrons which are slowed down mainly by collisions with the nuclei of the moderator. Their flux distribution varies inversely with the energy in the range from about 100 keV down to about 0.5 eV. The spectrum of the slowing down neutron is described in the ideal case by a $1/E$ dependence given by:

$$\varphi(E) \approx 1/E \tag{1.1}$$

But in actual irradiation site it can be replaced by:

$$\varphi(E) \approx 1/E^{1+\alpha} \tag{1.2}$$

With α greater or less than zero being to first approximation independent of neutron energy.

• Thermal or moderated neutrons. These neutrons, with energies below 0.5 eV, are in thermal equilibrium with the atoms of the moderator and show a Maxwellian distribution:

$$E(T) = kT \quad \text{or} \quad v(T) = [2E(T)/m]^{1/2} = [2kT/m]^{1/2} \tag{1.3}$$

With a most probable energy of 0.0253 eV at 20°C, (corresponding to mean neutron velocity of 2200ms^{-1})

The most commonly occurring nuclear reaction with neutrons is the neutron capture or (n,γ)-reaction with thermal and epithermal neutrons. The distribution of the reactor neutron spectrum varies in the irradiation sites of different research reactors and even in the different irradiation sites within the same reactor. It is therefore important to measure the neutron spectrum parameters. The resultant energy spectrum of neutrons is shown in Figure 1.1.

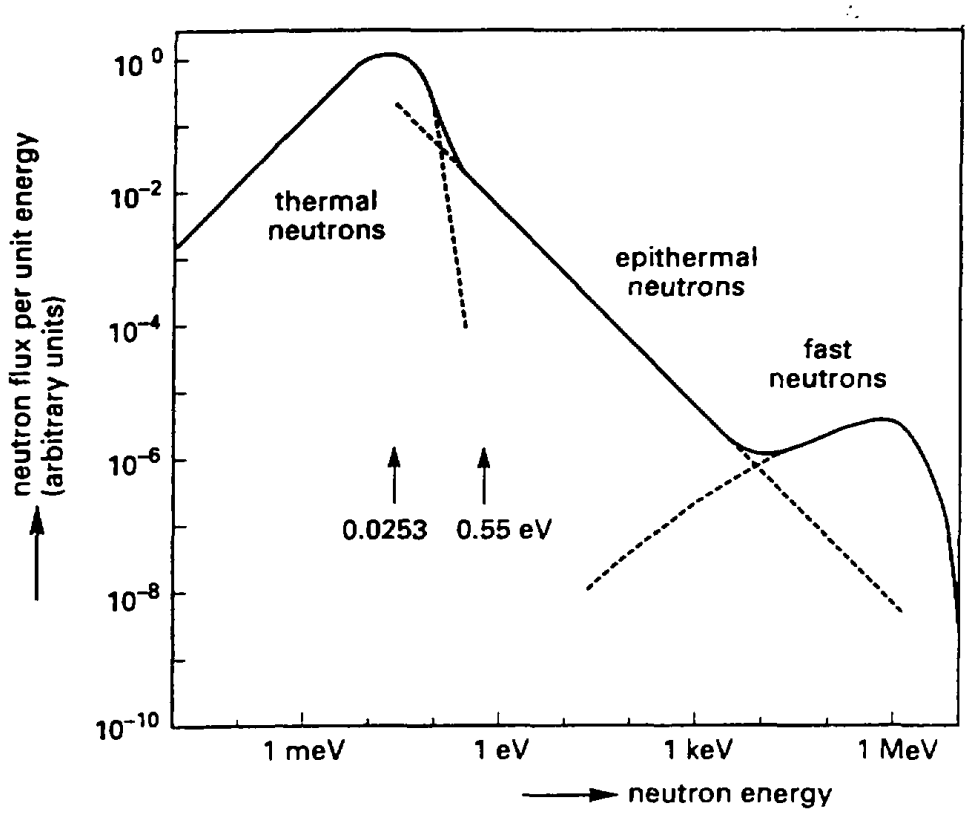


Figure 1.1: A Schematic neutron flux spectrum of a nuclear reactor (Stefaan *et al.,* 1991)

The thermal neutron component consists of low-energy neutrons which are in thermal equilibrium with atoms in the reactor's moderator. In most reactor irradiation channels, activation of samples occurs majorly through bombardment of the sample by thermal neutrons. The epithermal neutrons represent only a small fraction of total reactor neutrons. In practice the lower end of neutrons energy range used in Epithermal Neutron Activation Analysis (ENAA) is closer to 0.5eV which is the cadmium Cd cutoff energy (≈ 0.55 eV) while the higher end of the neutrons energy range extends through the resonance neutron region to several keV (Decorte, 1987, Verheijke, 1992, Glascock, 2004).

1.3 The Epithermal Neutron Flux Spectrum

In an ideal thermal neutron reactor, the thermal and epithermal neutron flux per unit energy interval is inversely proportional to the neutron energy at that interval.

$$\phi_{epi}(E) = \phi'_{epi}\frac{1}{E} \tag{1.4}$$

Where ϕ'_{epi} the energy independent proportionality constant, is the integrated epithermal neutron flux per unit of $\ln(E)$ interval for a $1/E$ epithermal neutron flux (Yücel and Karadag, 2004; De Corte, 1979).

This based on the assumption that the moderation process in an ideal reactor takes place in a homogeneous infinite medium, the sources of fission neutrons are homogeneously distributed throughout the moderator and that absorption, inelastic and anisotropic elastic scattering during moderation do not occur (Mukhin, 1970; Jovanovic *et al.,* 1987). However, for epithermal flux distribution in a 'real' reactor spectrum, this is an over assumption of the moderation situation. Moderation processes of the fission neutrons in the research reactor core vary from one research reactor to another and even in different

irradiation sites within the same type of research reactor due to factors that include the type of reactor, core configuration, type and geometry of the moderation materials, fuel distribution in the reactor core, types of reflector materials and geometry of the irradiation sites (Ryves, 1969; De Corte *et al*., 1979; Sheyin, 2015).

As a result of this variation, the epithermal neutron spectrum in actual irradiation sites may deviate from the ideal $1/E$ law. The non-ideal epithermal neutron flux distribution is better approximated as (De Corte *et al*., 1979;Yücel and Karadag, 2004):

$$\phi_{epi}(E) = \phi'_{epi}\frac{(1eV)^{\alpha}}{E^{1+\alpha}} \tag{1.5}$$

Where ϕ'_{epi} the energy independent proportionality constant is the integrated epithermal neutron flux per unit of $E^{-\alpha}/-\alpha eV^{\alpha}$ interval. The epithermal neutron flux shape factor α is an energy independent parameter which shows the degree of deviation of the non-ideal $1/E^{1+\alpha}$ epithermal neutron spectrum from the ideal $1/E$ epithermal neutron flux distribution in the actual reactor irradiation sites. Depending on the reactor configuration, the parameter α can either be positive or negative (De Corte *et al*., 1979; Yücel and Karadag, 2004).The epithermal spectrum in a well thermalized irradiation site is said to be softened and has a positive α-value, while the spectrum is said to be hardened and it has a negative α-value in a poorly thermalized site.

1.4 Principles of activation analysis

When a material is bombarded by a nuclear particle produced by a nuclear source (such as nuclear reactor and particle accelerator), some of the atoms present in the material will interact with bombarding particle. These atoms may be converted into different isotopes of the same element, depending on the nature of the bombarding particle. In many cases the produced isotopes are radioactive and are termed radioisotopes. When the material is

bombarded with neutrons, then the resulting activation process is called neutron activation.

Measurement of characteristic radiation from nuclides formed directly or indirectly by activation with neutrons as a result of neutron capture through the (n, γ) reaction is known as neutron activation analysis (NAA). The method relies on excitation by neutrons so that the product nuclide yields a radioactive nucleus which also de-excites by emission of one or more characteristic delayed gamma rays, but at a much lower rate according to the unique half-life of the radioactive nucleus and it is the measurement of gamma-rays emitted during the decay of this isotope after irradiation that forms the basis of neutron activation analysis. NAA has applications in chemistry but also in other research fields, such as geology, archaeology, medicine, environmental monitoring and even in the forensic science (Yavar *et al.*, 2011; Potts, 1987).

The two generally employed procedures are classified as:

(i) *instrumental neutron activation analysis* (INAA) also known nondestructive technique involves the irradiation and analysis of sample without undergoing any chemical treatment in the course of the analysis.

(ii) *radiochemical neutron activation analysis* (RNAA), which involves taking up irradiated samples into solution so that a chemical separation procedure may be carried out to isolate specific trace elements from the more active matrix. This latter procedure lowers detection limits by perhaps one to two orders of magnitude.

In NAA, the concentration of the element to be determined in a sample is normally obtained through: the relative, absolute and the single comparator methods. The relative method requires simultaneous irradiation counting of sample containing the unknown

nuclide with a standard of known nuclide concentration. This method requires the irradiation of multiple standards if the analysis of more than one nuclide in a sample is required. The absolute method involves the irradiation of the sample containing the unknown nuclide with one known standard, but it requires the precise knowledge of the nuclear parameters (i.e. M, θ, γ, σ_0, $I_0(\alpha)$, λ) of both measured sample and standard nuclides. The accuracy of this method is subject to the uncertainties associated with the nuclear constants used. The single comparator method represents an application of the absolute method to a single standard. The unreliable nuclear data are replaced by accurate experimentally determined compound nuclear constants called the *k*-factors. With the reactor parameters and counting conditions determined, the k_0- method (made possible by conversion of k-factors to k_0-factors) becomes a flexible single-comparator technique for which each sample is simultaneously irradiated with the chosen single comparator element. After irradiation, the comparator element can be used in routine measurements instead of separate standards for each element (Yavar *et al.*, *2011*, Glascock, 2004). Where the k_0-factor is expressed as:

$$k_0 = \frac{M_c \gamma_s \theta_s \sigma_{o,s}}{M_s \gamma_c \theta_c \sigma_{o,c}} \tag{1.2}$$

Once these factors are determined for a specific counting geometry, results of the same quality as those obtained with the relative method should be possible.

Where M, θ, γ, σ_0, λ, $I_0(\alpha)$ represents the atomic mass, isotopic abundance of the target isotope, gamma ray abundance, thermal neutron absorption cross section, decay constant and the α dependent resonance integral.

In addition, if the epithermal spectrum deviates from the ideal *1/E* behavior, the knowledge of the parameter *a* is required. The single comparator method is best suited for well thermalized irradiation sites where the flux does not vary significantly with time. Because of its experimental simplicity, the application of this method when a large number of nuclides are analyzed is very useful (De Corte 1987; Greenberg *et al*., 2011; Yavar *et al.*, 2011).

1.5 Aim and Objectives

The aim of the work is to re-characterize one outer (B_4) and one inner (B_2) irradiation channels of NIRR-1 before conversion.

The objectives of this work are to:

i. Experimentally determine the degree of deviation of the epithermal neutron flux (α), in two irradiation channels of NIRR-1
ii. Calculate the ratio of thermal to epithermal flux *(f),* inside channels B_2 and B_4 of NIRR-1.
iii. Compare the α and *f* values obtained with those at the commission of the reactor.
iv. Provide a baseline data for the development of protocols for the use of NIRR-1 for NAA after conversion from HEU to LEU.

1.6 Justification

NIRR-1 is designed for use in Neutron Activation Analysis, the need for a detailed knowledge of the neutron flux parameters in the irradiation sites is essential for experiment and benchmarking the simulation of reactor models. Over time these values deviate due to core modifications and ageing. Therefore the need to re-characterize the sites becomes imperative.

1.7 Previous Work

In 2005, Jonah *et al.* used the Cd-ratio for multi-monitor method to determined neutron spectrum in inner (B_2) and outer (B_4) irradiation channels of NIRR-1 after it was commissioned. Where they found out that their results were comparable with those of other reactor facilities, which have similar core configuration.

For the purpose of adopting the k_0- standardized NAA method in NIRR-1, Sadiq *et al* ; (2010), characterized one inner (A_1) and one outer (A_2) irradiation channels of NIRR-1 using "Cd Ratio multi monitor" . Where he compared the result obtained was in good agreement with previously reported value reported by Jonah, 2005 and with those reported from other MNSR's with similar core configurations except for the deviation in the α-value for the inner irradiation channel of Ghana Research Reactor 1 (GHARR-1).

After complete core conversion of the Dalat Nuclear Research Reactor (DNRR) to low enriched uranium (LEU) in 2014, Vu *et al.,* re-established the neutron spectrum parameter and it was observed that the thermal neutron flux in most of the irradiation channel decreased by 6-9% while the epithermal neutron flux increased by 2-6%. From his investigation, he found out that the neutron spectrum in the irradiation channels were hardened.

In order to determine the consistency in the neutron flux parameters in application for k_0 measurements, Şahin in 2014 re-evaluated the neutron flux characterization parameters for the pneumatic rabbit facility RT-2 at the National Bureau of Standards Reactor, using cadmium-covered and bare foil measurements and a reactor simulation code MCNP to quantify the measure of the non-ideal epithermal neutron flux distribution (α) and the thermal to epithermal neutron flux ratio *(f)* , the results showed that the bare foil measurements were not found physically reasonable and consistent when applying the

‘‘bare-triple-monitor method’’ and ‘‘bi-isotopic method’ compared to the Cadmium-covered foil measurements and the computational method which proved to be consistent with the previously measured values.

In 2002, Akaho *et al.,* determined the spectral indices and neutron temperatures of the inner and outer irradiation sites of GHARR-1 using the cadmium ratio method. They found out that the computed modified spectral indices using nuclides of different Q_0-values were generally in good agreement with the measured values for the irradiation sites of reactors with different f-values within the range of 18.2 - 152. However, he attributed some discrepancies observed to the choice of monitor and cut-off energy parameter, and he suggested that appropriate correction factors could be used to obtain calculated values to agree favorably with experimental values.

Sheyin in 2015, used cadmium covered multi-monitor method to characterized permanent cadmium lined irradiation channel installed in the large outer irradiation site of the NIRR-1 in order to determine the value of the epithermal neutron shape factor (α). He concluded the the epithermal neutron spectrum in the channel is poorly thermalized.

De Wispelaere *et al.,;*(2006), re-evaluated the neutron flux parameters in channels Y4 and S84 of the Belgian reactor 1 (BR1) reactor using Cd-ratio for multi-monitor method and bare triple-Monitor. Where they concluded that the discrepancy between the new data and the old data may be explained by the fact that the cadmium ratio for multi-monitor method used leads to more accurate results but for the bare triple-monitor result the difference can probably be found in the fact that the nuclear data for the Zr-isotopes were extensively re-investigated and they differ significantly from the data used in the earlier.

Ahmed, 2004 characterized two irradiation sites (Channels No.5 and No.7) of Ghana Research Reactor-1 (GHARR-1) using cadmium cover method, where he showed that the

thermal to epithermal flux ratio *(f)* the epithermal flux-shaping factor α for the characterized channels in good agreement with previous values determined by Akaho 2002.

Njinga *et al,;* (2012) performed measurements using Cu-wires and (0.1)%Au-Al foils on the installed permanent Cd-lined irradiation channel in one of the large outer channel of NIRR-1 for use in epithermal and fast NAA procedures to characterize the thermal, epithermal column and check its effect on the neutron flux distributions via the specific activities obtained using (n,γ), (n,p) and (n,α) reactions in other channels shows that the flux distributions have not been affected by the Cd-liner in outer channel A-3.

After 10 years operation Of Pakistan Research Reactor-2 (PARR-2), a miniature neutron source reactor (MNSR), a beryllium reflector was added to compensate the loss of reactivity due to burn up of fuel. Measurement of important Parameters such as effective delayed neutron fraction, decay constant, excess reactivity, control rod worth, temperature coefficient of reactivity, thermal neutron flux, cadmium ratio were done after the addition of Be reflector. Neutron flux measurements were carried out using thin gold foils of 50 mm thickness and 99.99% purity (Masood Iqbal *et al* 2002).

After over 10 years of operation of Ghana Research Reactor-1 (GHARR-1), the total neutron flux was measured after a beryllium reflector was added to its shim to compensate for loss of excess reactivity. The thermal, epithermal and fast neutron fluxes were determined by the method of foil activation. The experimental samples with and without a cadmium cover of 1-mm thickness were irradiated in the isotropic neutron field of the irradiation sites of GHARR-1 facility. The induced activities in the sample were measured by gamma ray spectrometry with a high purity germanium detector (Sogbadji *et al* 2011).

As the NIRR-1 core is mainly designed for neutron activation analysis, there is need for a detailed information on the neutron flux parameters so as to enhance the application of the reactor in its application. And with the imminent conversion of the core from HEU to LEU the neutron flux parameters will help in developing new analytical protocols or fine tuning the old protocols so as to be used in NAA after coversion.

CHATER TWO

LITERATURE REVIEW

2.1 Sources of Neutrons

A neutron source is any device with which neutrons are produced, irrespective of the mechanism used in the process of the neutrons production. Neutron sources can be distinguished from one another by the rate at which neutrons are emitted, energy of the neutrons emitted and size of the source. These neutron sources are the basic essentials required to carry out neutron activation analysis.

The three main sources of neutrons are:

- Isotopic neutron sources including Radioisotope Sources ((α,n) and (γ,n) reactions, spontaneous fission and photo neutron sources
- Accelerators based sources including ion and electron accelerator and neutron generators
- Nuclear Research Reactor (nuclear reactors used as neutron sources);

Research nuclear reactors have the highest neutron fluxes, but are limited concerning on-site determination, price, and availability. Consequently, nuclear reactors are used predominantly for neutron activation analysis of very minute amounts or for sensitive neutron radiography. In cases of on-site irradiation, neutron generators or isotopic sources are used (Alafasi *et al.*, 1995; Ahmed, 2004; Murugeshan, 2009).

2.1.1 Nuclear Reactors

These are the commonly used source of neutrons for activation analysis. Most research reactors depend on the fission of ^{235}U. This isotope is naturally radioactive, with a half-life of 7.038×10^8 years, and will spontaneously decay by nuclear fission, in which the nucleus splits into isotopic fragments, releasing high-energy neutrons and energy. The

cross-section for neutron induced fission of fissionable nuclides increases with decreasing energy of the neutrons, in order to increase the neutron activity, moderators that slowed down the neutrons are added to the reactor. Nuclear reactors are categorized according to their fuel, moderator, coolant, reflector, and configuration. Examples of nuclear reactors are TRIGA Reactors, SLOWPOKE and the Miniature Neutron Source Reactor (MNSR) (Alafssi *et al.*,1995; Ahmed, 2004).

2.1.2 Description of NIRR-1

The Nigeria Miniature Neutron Source Reactor, code-named; Nigeria Research Reactor-1 (NIRR-1), is a low-power research reactor with nominal thermal power of 31 kW. It is a small, safe nuclear facility that employs highly enriched uranium as fuel, light water as moderator/coolant, and beryllium as reflector. The reactor is designed, manufactured and installed by China Institute of Atomic Energy (CIAE), Beijing, China. It is designed for use in universities, hospitals and research institutes mainly for Neutron Activation Analysis, limited production of short-lived radioisotopes and training (SAR, 2012).

Similar to the Canadian SLOWPOKE, NIRR-1 is a tank-in-pool type research reactor, low power which uses highly enriched uranium as a fuel, light water as moderator and beryllium as reflector. Heat generated in the core is removed through a natural convection process and is transferred to the pool water through vessel walls. The beryllium reflector in' the reactor can be divided to three types: the side annulus reflector surrounding the reactor core, the bottom plate, and the top beryllium shims. The side reflector is an annular cylinder of 23.1 cm inner diameter, 43.5 cm outer diameter, and 23.85 cm in height (SAR, 2012). The bottom reflector is a disc 29.0 cm in diameter and 5.0 cm in thickness. The top reflector is composed of a group of semicircular beryllium shims with different thickness, with 24.3 cm in diameter. There are 46 shim plates giving a total thickness of

10.95 cm. These beryllium shims are used to compensate the reactivity losses caused by fuel burn-up and poisoning buildup of xenon and samarium during the reactor operation. NIRR 1 has ten irradiation sites, five are called " inner " and uniformly located inside the beryllium annulus reflector while the other five are called " outer " and surround the annulus reflector externally. The maximum thermal neutron flux in the inner and the outer sites is $1.0x10^{12}$ and $5.0x10^{11}$ $ncm^{-2}s^{-1}$, respectively. The nominal thermal power of the reactor at this neutron flux level is about 30 kW. The total excess reactivity of the core was limited to less than 4 mk when the reactor was commissioned using reactivity regulators (SAR, 2012; Jonah *et al.*, 2005; Ahmed, 2004).

The core itself is undermoderated with HEU ratio of 197 and also due to orificing effect, the MNSR system has negative temperature coefficient of reactivity with value 0.132 mk/^{o}C in 25-32^{o}C range. In case of uncontrolled power excursion, it has self-limiting peak power value of 87 kW.The reactor core is suspended inside a 0.65 m diameter reactor vessel, immersed in a 6×3.5×7 m water pool. A longitudinal section view at the core is shown in Figure 2.1 and the main specifications of NIRR-1 are shown in Table 2.1.There are other auxiliary systems for the utilization of the reactor such as the pneumatic transfer systems. The system known as type A is suitable for irradiation for medium and long time. Type B, a multifunction capsule transfer system, is coupled to four irradiation tubes.

NIRR-1 core is a small compact system consisting of a central control rod guide tube, the fuel cage and fuel pins arranged in ten concentric lattice rings about the control guide tube. The average radial pitch between any two adjacent fuel rings is 10.95mm (Jonah *et al*, 2005, SAR 2012, Ahmed *et al*, 2004).

Table 2.1: Main Specifications of NIRR-1

Item	**Description**
Type	Tank-in-pool
Nominal core power	31 kW (th)
Coolant/Moderator	de-ionized light water
Loading of U-235 in core	1006.65 g
Reflector	Metallic beryllium
Excess Reactivity-cold, clean	3.77 mk
Daily operation fluence in inner irradiation sites	$< 9 \times 10^{15}$ cm^{-2}
Fuel life in core	$> 3.24 \times 10^{19}$ cm^{-2}
Neutron flux at inner irradiation sites	1×10^{12} $cm^{-2}s^{-1}$, stability □ 1 %, horizontal and vertical variation < 3 %
Number of irradiation sites	10 sites (5 inner and 5 outer) 6 sites connected (4 inner and 2 outer)
Control rod	1, Stainless steel clad, Cadmium absorber
Reactor operation mode	Manual and automatic
Temperature in irradiation sites	Inner site < 54 ^{0}C; outer sites < 40 ^{0}C (at pool temperature of 20 ^{0}C).
Core reactivity temperature coefficient	-0.1 mk/^{o}C; for core temperature 15-40 ^{o}C
Average radiation dose in reactor hall	< 1 μSv/h

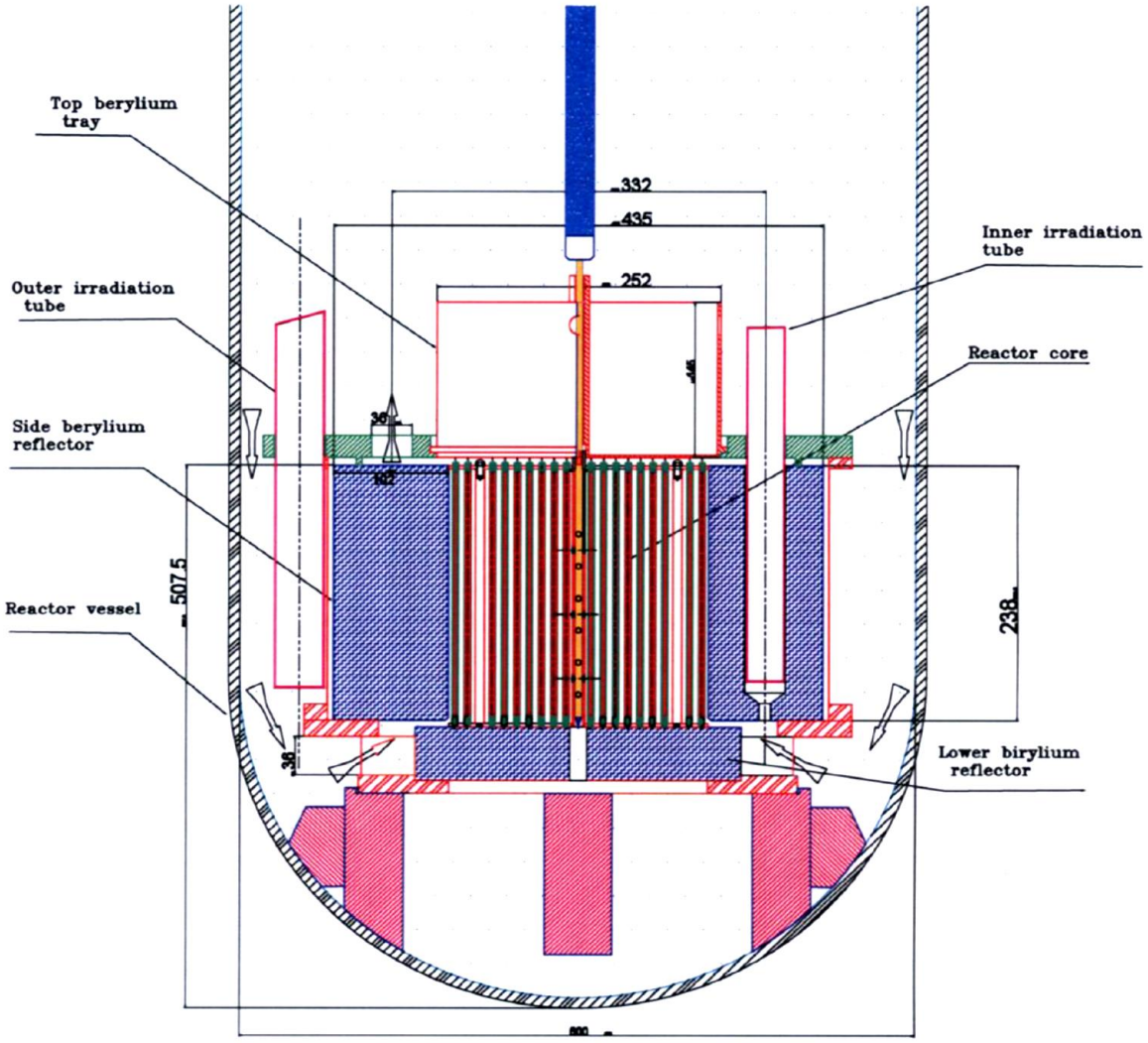


Fig.2.1: Schematic longitudinal section of MNSR vessel (Hainoun and Alhabit, 2007)

2.2 Neutron Activation Analysis

Neutron activation is a method of elemental analysis based on the measurement of characteristic radiation from nuclides formed directly or indirectly by activation with neutrons. This method is based on the conversion of a stable nucleus ${}^{A}_{z}X$ into a radioactive one by neutron capture, forming a compound nucleus (${}^{A+1}_{z}\overline{X}$) with an extra neutron and entering excited state (Verheijke, 1992). This excited compound nucleus will almost instantaneously de-excite into a more stable nucleus (${}^{A+1}_{z}X$) through the emission of one or more characteristic 'prompt radiations', immediately after the capturing neutron. These prompt radiations can be an α-particle, a proton, a neutron, a γ-ray photon or another type of radiations depending on the energy of the incident neutrons.

When the main reaction occurred with low-energy neutrons, an (n, γ) reaction is formed. This is the case in which, the highly energetic level of the compound nucleus is de-excited by emission of prompt γ-rays. On the other hand, when high-energy neutrons are absorbed it results in the ejection of a particle i.e. a proton, a neutron, or an α-particle (Potts, 1987). The newly formed nucleus, produced upon the de-excitation of the compound nucleus, may be unstable. When unstable, already during activation it starts to decay with half-life ranging from fractions of a second to many years to a stable state by emission of specific radiation 'delayed emission 'through one or more of the following processes: α-decay, β^- -decay, β^+-decay, or internal transition decay. In most cases, delayed γ- and X-rays will be emitted too. This decay process is at a much slower rate than the initial de-excitation and is dependent on unique half-life of the radioactive nucleus. Measuring the emitted radiations, prompt and/or delayed, (using a suitable radiation detector) leads to identification of the isotopes, resulting upon irradiation with neutrons, and thus of parent elements and their concentration levels **(**Kubešová, 2012; Soliman, 2012, Franca, 2012**)**.

During activation, two processes occur: formation of radioactive nuclei by activation, and also decay of these nuclei. The results of the two processes are combined in the basic activation formula for the activity "*A"* of a radionuclide formed through a specified reaction.

Neutron activation analysis is usually carried out with thermal neutrons through the reaction given as:

$$ {}^{A}_{Z}m\left(n,\gamma\right){}^{A+1}_{Z}m \tag{2.0} $$

If the target sample contain N number of nuclei per volume (cm^3) in a neutron flux $\left(\Phi\right)$, then the number of interaction I_N will be expressed as;

$$ I_N = \phi\sigma N(cm^{-3}.s^{-1}) \tag{2.1} $$

From this, the samples of N_p nuclei with cross-section σ, irradiated in a constant neutron flux ϕ during an irradiation time t_{irr} according to the reaction;

$$ N_p \xrightarrow{\sigma\phi N_p} N_d \xrightarrow{\lambda N_d} N_s \tag{2.2} $$

where N_p, N_d, N_s are the parent, daughter and stable nuclei, σ is the reaction cross section and λ the disintegration constant $\left(s^{-1}\right)$ then if N_p is considered constant, then the rate of forming a daughter nuclei is given as (Franca . 2012);

$$ \frac{dN_s}{dt} = N_p\phi\sigma_p - \lambda_d N_d \tag{2.3} $$

From which N_d can be evaluated by integrating $t = 0$ from to t_{irr}, thus;

$$ N_d = \frac{N_p\phi\sigma}{\lambda_d}\left[1 - e^{-\lambda_d t_{irr}}\right] \tag{2.4} $$

The decay constant is related to the commonly used half-life according to:

$$\lambda = \frac{\ln 2}{t_{1/2}} = \frac{0.639}{t_{1/2}} \tag{2.5}$$

The activity of N_d can be defined after an irradiation time t_{irr} as;

$$A = \lambda_d N_d = N_p \phi \sigma \left[1 - e^{-\lambda_d t_{irr}}\right] \tag{2.6}$$

Activation of a sample by neutrons is the first stage in NAA. The growth of the number of radioactive nuclei during irradiation with mono-energetic neutrons is expressed as:

$$\frac{dA_i}{dt} = RN_0 - \lambda N_i \tag{2.7}$$

where $A_i(t) = \lambda N_i$

The number of target atoms of the considered (n, γ) reaction in a given sample is given by:

$$N_0 = \frac{wN_A\theta}{M} \tag{2.8a}$$

Where w, is the weight of the element in the sample, N_A is the Avogadro's number and M is the atomic weight of the nuclei and Θ is the isotopic abundance.

Integrating equation (2.7) over the irradiation time yields the number of radioactive nuclei at the end of the irradiation period.

$$N(t) = \frac{RN_0}{\lambda}(1 - e^{-\lambda t_{irr}}) \tag{2.8b}$$

2.3 Reaction Rate

Knowledge of the neutron flux (ϕ) and the material cross sections allows the computation of the rate of interactions. The reaction rate, *RR* [reactions/cm^3·sec], is centered on the total number of neutron-nucleus interactions

$$RR = (nv)N\sigma = \phi(N\sigma) = \phi\sum \tag{2.9a}$$

The reaction rate per nucleus of isotopes undergoing a certain neutron flux is given by (Stefaan *et al.*, 1997):

$$R = \int_0^\infty n(v)v\sigma(v)dv = \int_0^\infty \phi(v)\sigma(v)dv = \int_0^\infty \phi(E)\sigma(E)dE \tag{2.9b}$$

In principle the reaction rate is calculated from numerical integration of the product of the energy/velocity dependent neutron flux and (n,γ) cross section (equation 2.9a). The impracticality of the procedure lead to the adoption of convention in order to simplify the calculation of the reaction rate. For the purpose of this research the Hogdahl convention is adopted, as it deals with the contribution of the thermal neutron and that of the epithermal neutrons separately. Equation (2.7) becomes (Greenberg *et al.*, 2011):

$$\frac{dA_i}{dt} = N_0\int_0^\infty \phi(E)\sigma(E)dE - A_i(t) \tag{2.11}$$

With correction for decay after irradiation and conversion of *N* to the corresponding concentration of an element in a sample yield (Verheijke, 1992):

$$A_i(t,T) = \frac{N_A\theta wa}{M}\int_0^\infty \varphi(E)\sigma(E)dE\cdot(1-e^{-\lambda t_{irr}})e^{-\lambda t_d} \tag{2.12}$$

Where w, Θ, a M, N_A, t_{irr} and t_d are the weight of the irradiated element, isotopic abundance of the target isotope, abundance of the considered γ-ray, atomic mass of the irradiated element, Avogadro's number, irradiation time and decay time respectively.

Equation (2.12) applies to the direct formation of radionuclides. For indirect formation through decay or activation of one of the activation products different formulas have to be used.

2.4 Thermal and epithermal activation

In neutron activation analysis the division between thermal and epithermal neutrons is at the cadmium cut-off energy (E_{cd}) of 0.55 eV. This is the recommended value for a cylindrical cadmium box with a uniform thickness of 1 mm is 0.55 eV (Decorte, 1987; Potts, 1987). The reaction rate per nucleus according to equation (2.10) can be written as

$$R = \int_0^\infty n(\mathrm{v})\,\mathrm{v}\,\sigma(\mathrm{v})\,\mathrm{dv} \tag{2.13a}$$

With

$$\phi = nv \tag{2.13b}$$

where R, v, $n(v)$, $\sigma(v)$ and v_{cd} are reaction rate per nucleus, neutron velocity, neutron density as function of velocity, neutron activation cross-section, neutron velocity corresponding to E_{cd}.. According to the Hogdahl's convention, the reaction rate can be splitted into *thermal* and the *epithermal* reaction rates i.e.:

$$R = \underbrace{\int_0^{v_{cd}} n(\mathrm{v})\,\mathrm{v}\,\sigma(\mathrm{v})\,\mathrm{dv}}_{a} + \underbrace{\int_{v_{cd}}^\infty n(\mathrm{v})\,\mathrm{v}\,\sigma(\mathrm{v})\,\mathrm{dv}}_{b} \tag{2.14a}$$

The second part of equation (2.14a) becomes

$$\int_{v_{cd}}^{\infty} n_n(\mathrm{v}_n)\,\mathrm{dv}_n = \phi_{epi} \int_{E_{cd}}^{E_{\max}} \frac{\sigma(\mathrm{E}_n)\,\mathrm{dE}_n}{E_n} \tag{2.14b}$$

where, E_n ,E_{max}, ϕ_{epi} represents the neutron energy, maximum energy of the epithermal neutrons(1 to 2 Me V), conventional epithermal neutron flux respectively.

For the thermal part of equation (2.14), where $\mathrm{v} < \mathrm{v}_{\mathrm{Cd}}$, it is convenient to consider the neutron flux as a product of the neutron density and the velocity, since the epithermal flux is inversely proportional to the energy, the integration of the second term (b) is carried out with respect to the energy (Greenberg *et al.*, 2011):

$$R = \sigma_o v_0 \int_0^{v_{cd}} n_n(\mathrm{v}_n)\,\mathrm{dv}_n + \phi_{epi} \int_{E_{cd}}^{E_{\max}} \frac{\sigma(\mathrm{E}_n)\,\mathrm{dE}_n}{E_n} \tag{2.15}$$

where, v_0 is the most probable neutron velocity at 20ºC and 2200 m s^{-1}, and σ_o is the thermal neutron activation cross-section for the corresponding energy, 0.0253 eV,

$$n = \int_0^{\infty} n(\mathrm{v})\,\mathrm{dv} \Rightarrow n_{th} = \int_0^{v_{cd}} n(\mathrm{v})\,\mathrm{dv} \tag{2.16}$$

with n_{th} as the thermal neutron density (where $\phi_{th} = \sigma_o n_{th}$), and ϕ_{th} is the conventional thermal neutron flux, for energies up to the Cd cut-off energy.

Then equation (2.14a) becomes

$$R = \phi_{th}\sigma_o + \phi_{epi} \int_{E_{cd}}^{E_{\max}} \frac{\sigma(\mathrm{E}_n)\,\mathrm{dE}_n}{E_n} \tag{2.17}$$

Therefore, the thermal reaction rate is given by the first part of equation (2.17) .i.e.

$$R_{th} = \phi_{th}\sigma_o \tag{2.18}$$

2.4.1 The epithermal reaction rate

The epithermal neutron flux per unit energy interval is generally accepted to be inversely proportional to the neutron energy, "*E"* (De Corte *et al*., 1979a; De Corte *et al*., 1979b, De Corte *et al*., 1981; Yücel and Karadag, 2004):

$$\phi_{epi}(E) = \phi'_{epi}\frac{1}{E} \tag{2.19a}$$

With resonance integral for a 1/E epithermal neutron spectrum defined as:

$$I_o = \int_{E_{cd}}^{E_{\max}} \frac{\sigma(E_n)dE_n}{E_n} \tag{2.19b}$$

Where

I_o = the infinite dilution resonance integral including $1/v$ tail of thermal neutron spectrum or the epithermal neutron absorption cross section.

$\sigma(E_n)$ = the cross section as a function of energy E

Another important parameter is the cross section ratio *(Q_0)* (i.e. the ratio of resonance integral to (n,γ) cross section at a 2200 m s-1 neutron velocity), which is defined in the ideal $1/E$ spectrum as:

$$Q_0 = \frac{I_0}{\sigma_0} \tag{2.20}$$

The reaction rate for an ideal $1/E$ epithermal spectrum may be determined by:

$$R_{epi} = \int_{v_{cd}}^{\infty} n_n(\mathrm{v}_n)\,\mathrm{dv}_n = \phi_{epi}\int_{E_{cd}}^{E_{\max}} \frac{\sigma(\mathrm{E}_n)\,\mathrm{dE}_n}{E_n} \tag{2.21a}$$

$$R_{epi} = \phi_{epi} I_o \tag{2.21b}$$

From equation (2.20), the epithermal neutron absorption cross-section or resonance integral (I_o) is defined as equation (2.19b) is an essential nuclear parameter in neutron activation as it helps in the determination of the reaction rate with respect to epithermal neutrons. The definition of the resonance integral in equation (2.19b) shows that the energy dependence of epithermal neutron flux density is proportional to $1/E$.

In actual irradiation sites the epithermal neutron flux deviate from the ideal $1/E$ law and it is in most cases approximated as (De Corte *et al*., 1979a; De Corte *et al*., 1979b, De Corte *et al*., 1981, Yücel and Karadag, 2004):

$$\phi_{epi}(E) = \phi'_{epi} \frac{(1eV)^{\alpha}}{E^{1+\alpha}} \tag{2.21}$$

Since the definition of the resonance integral equation (2.19b) holds for the ideal epithermal spectrum ($1/E$), then it should be corrected for the actual epithermal spectrum ($1/E^{1+\alpha}$):

$$I_0(\alpha) = (1\mathrm{eV})^{\alpha} \int_{E_{cd}}^{E_{max}} \frac{\sigma(\mathrm{E}_n)(1eV)^{\alpha}\, \mathrm{dE}_n}{E_n^{1+\alpha}} \tag{2.22}$$

where $I_0(\alpha)$ is the resonance integral for a non-ideal epithermal neutron spectrum. The resonance integrals defined by equation (2.22) can be used in the calculation of the epithermal activation in a particular irradiation position, characterized by α. For simplicity the reference energy $(1\mathrm{eV})^{\alpha}$ may be omitted (ie. $(1\mathrm{eV})^{\alpha} \equiv 1$) in order to obtain the relationship between I_0 and $I_0(\alpha)$. If $\bar{E}_r$ and α are known, it is possible to convert I_0,

as tabulated in literature to $I_0(\alpha)$ by equation (2.23) (De Corte *et al*., 1979b, 1981, Yücel and Karadag, 2004):

$$I_o(\alpha) = \left[\frac{(I_o - 0.429\sigma_o)}{(\bar{E}_r)^{\alpha}} + \frac{0.429\sigma_o}{(2\alpha+1)(E_{cd})^{\alpha}} \right] \cdot (1eV)^{\alpha} \tag{2.23}$$

where the term $(I_0 - 0.4264\sigma_0)$ represents the reduced resonance integral (i.e. with $1/v$ tail subtracted) and equation 2.23 is only valid for $E_{cd} = 0.55eV$, since $0.4264 = 2(E_o/E_{cd})^{1/2}$ with the most probable neutron energy at 20°C $E_o = 0.0253$ and $E_{cd} = 0.55eV$.

The effective resonance energy $\bar{E}_r$ represents the energy of a single effective or average energy which replaces all the resonance energies of an isotope over the epithermal neutron energy region (Ryves, 1969). It is defined experimentally by an α dependent parameter as (Ryves, 1969; Jovanovic*et al*., 1987; Moens *et al*., 1979):

$$(\bar{E}_r)^{-\alpha} = \frac{I'_o(\alpha)}{I'_o} \tag{2.24}$$

Where I'_o and $I'_o(\alpha)$ are the reduced resonance integrals (tail subtracted) for $1/E$ and $1/E^{1+\alpha}$ epithermal spectra respectively (Moens *et al.,* 1979; De Corte *et al*., 1981,).

$$I'_o = \int_{E_{cd}}^{\infty} \left[\sigma(E) - \frac{\sigma_o v_o}{v} \right] \frac{dE}{E} \tag{2.25a}$$

$$= \int_{E_{Cd}}^{\infty} \sigma(E) \frac{dE}{E} - \int_{E_{Cd}}^{\infty} \frac{\sigma_o v_o}{v} \frac{dE}{E} = I_o - \int_{E_{cd}}^{\infty} \frac{\sigma_o v_o}{v} \frac{dE}{E}$$

$$= I_o - 2\sigma_o \frac{(E_o)^{1/2}}{(E_{Cd})^{1/2}}$$

$$= I_o - 0.4264\sigma_o \tag{2.25b}$$

and

$$I'_o(\alpha) = \int_{E_{cd}}^{\infty} \left[\sigma(E) - \frac{\sigma_o v_o}{v} \right] (1eV)^{-\alpha} \frac{dE}{E^{1+\alpha}} \tag{2.26a}$$

$$= I_o(\alpha) - \int_{E_{cd}}^{\infty} \frac{\sigma_o v_o}{v} \frac{dE}{E} (1eV)^{-\alpha} \frac{dE}{E^{1+\alpha}}$$

$$= I_o(\alpha) - \sigma_o \frac{(1eV)^{-\alpha} \sqrt{E_o}}{(\alpha + 1/2)(E_{Cd})^{\alpha+1/2}}$$

$$= I_o(\alpha) - \sigma_o \frac{0.4264(1eV)^{-\alpha}}{(2\alpha+1)(E_{Cd})^{\alpha}} \tag{2.26b}$$

Also Q_0 can be converted to $Q_0(\alpha)$ by equations 2.27a and 2.27b

$$Q_o(\alpha) = \frac{I_o(\alpha)}{\sigma_o} = \frac{(1\text{eV})^{\alpha}}{\sigma_o} \int_{E_{cd}}^{E_{\max}} \frac{\sigma(\mathrm{E}_n)\,\mathrm{dE}_n}{E_n^{1+\alpha}} \tag{2.27a}$$

$$Q_{o,i}(\alpha) = \left[\frac{Q_{o,i} - 0.429}{(\bar{E}_{r,i})^{\alpha}} + \frac{0.429}{(2\alpha+1)(E_{cd})^{\alpha}} \right] \cdot (1eV)^{\alpha} \tag{2.27b}$$

$Q_o(\alpha)$ can be easily calculated from Q_o if α is known and the effective resonance energy, E_r is available. Both E_r and Q_o values are tabulated in work of Decorate and Simonitis as nuclear constants and applicable to all practical irradiation condition. The effective resonance energy E_r must be used for the correction of resonance integrals in deviating epithermal spectrum. It is the energy of a single resonance which gives the same resonance activation effect as the actual resonances for the isotopes. Where E_r is defined as:

$$(E_r)^{-\alpha} = \frac{I_o(\alpha)}{I_o}(1eV)^{-\alpha} \quad (2.27c)$$

According to equation (2.17), the expression for the reaction rate can therefore be re-written as

$$R = \phi_{th}\sigma_o + \phi_{epi}I_o(\alpha) \quad (2.28a)$$

Equation (2.28a) can be rearranged to:

$$R = \phi_{th}\sigma_o(1 + fQ_o(\alpha)) \quad (2.28b)$$

where

$$f = \frac{\phi_{epi}}{\phi_{th}} \quad (2.28c)$$

From equation (2.28b) an effective cross-section (σ_{eff}) can be defined as:

$$\sigma_{eff} = \sigma_o(1 - fQ_o(\alpha)) \quad (2.29)$$

So, Equation (2.28a) can be simplified to:

$$R = \phi_{th}\sigma_{eff} \quad (2.30)$$

Since the contribution of the epithermal activation can be considerable, for some (n,γ) reactions and it even overshadows the thermal activation thus, we take account of the epithermal activation by the use of the *effective,* instead of the *thermal* cross-section, since the flux ratio (*f),* is present in the correction term (Verheijke, 1992, De Corte, 1981).

2.5 The activation formula

The activation formula is the basic expression for the determination of an element by means of an (n, γ) reaction and γ-ray spectrometry. The activation formula includes the decay after irradiation and the detection efficiency of the γ-rays, hence it is said to be a practical extension of equation (2.12). We relate the activation to the *thermal* neutron

flux, the correction for epithermal neutron activation being accounted for in the already defined *effective* cross-section (σ_{eff}). The activation formula is given by:

$$A = \frac{N_A \theta w}{M} \phi_{th} \sigma_{eff} SDCa\varepsilon \tag{2.31}$$

where the term *S* is called the saturation factor usually denoted by $(1-e^{-\lambda t_{irr}})$ and it expresses the fraction of the maximum radioactivity produced in time, t_{irr}. D and C represents the decay factor denoted by $e^{-\lambda t_d}$ and $(1-e^{-\lambda t_m}/\lambda t_m)$ with t_{irr}, t_d, and t_m as the irradiation respectively, decay, and measuring time respectively. While *a* is the abundance of the considered γ-ray, photons/disintegration, ε is the *detection* efficiency of the considered γ-ray at full energy peak.

2.6 Radiation Measuring Devices

The measurement of gamma rays from radioactive samples is usually done with an instrumentation which generally consists of a semiconductor detector, associated electronics, and a computer-based, multi-channel analyzer (MCA/computer). The most commonly used detector is the high purity or intrinsic germanium (HpGe) detectors, which operate at liquid nitrogen temperatures (77ºK) in order to minimize electronic noise created by the thermal excitation of electrons from valence to conduction bands. The most common type of HpGe detector is the coaxial detector, which in NAA is useful for measurement of gamma-rays with energies over the range from about 50 keV to 3.0 MeV (Glasscock, 2004; Ahmed, 2013).

The detector's energy resolution is a measure of its ability to separate closely spaced peaks in a gamma spectrum. In general, detector resolution is specified in terms of the Full Width at Half Maximum (FWHM) of the 122-keV photopeak of ^{57}Co and the 1332-keV photopeak of ^{60}Co. For most NAA applications, a detector with 1.0-keV resolution or

below at 122 keV and 1.8 keV or below at 1332 keV is sufficient (Glasscock, 2004; Ahmed, 2013).

2.7 Sensitivities & Detection Limits

The accuracy and sensitivities of Neutron Activation Analysis are dependent on the concentration of a particular element and radionuclide parameters (i.e., parent isotope abundance, neutron cross-section, half-life, and gamma ray abundance). The detection limit in NAA is based on the signal-to-noise ratio, the selectivity of determining, with a certain degree of confidence, a peak in the gamma-ray spectrum. The photopeak in the spectrum of the gamma-ray emission by the radionuclide of interest is the 'signal'. The 'noise' fallouts from the detection of photons from the ambient background, from the Compton continuum due to the interaction of higher energy γ-rays, as well as from γ-ray spectrum interferences from e.g. the blank from pre-irradiation treatment, from packing materials and from overlapping peaks. The detection limit depends on the irradiation, the decay and the counting conditions. It is quite common to estimate the detection limit using Currie's formula (Greenberge *et al.*, 2011;Glasscock, 2004).

$$D_L = 2.71 + 4.65\sqrt{B} \tag{2.32}$$

Where D_L is the detection limit and B is the background under a γ-ray peak. This approach is valid only when the γ-ray background (counting statistical error) is the major interference (Glasscock, 2004).

CHAPTER THREE

MATERIALS AND METHODS

3.1 Materials

The material used in carrying out this work are the irradiation facility, Pneumatic Transfer Systems, Polythene Vials, 1mm thick Cadmium, Digital weighing balance and Activation foils.

3.1.1 The irradiation facility

NIRR-1 consists of five small rabbit tubes installed inside the beryllium annulus known as the inner irradiation channels. Three small and two large rabbit tubes installed outside of the beryllium annulus known as the outer irradiation channels. Six out of the ten irradiation sites are presently connected to the pneumatic transfer systems.

3.1.2 Pneumatic Irradiation Rabbit Transfer System (PIRS)

Short time neutron activation analysis is carried out using pneumatic irradiation rabbit system (PIRS) installed at the (NIRR-1). There are two sets of transfer systems, the pneumatic transfer system type A and B (Jonah *et.al.* 2005). These provide a means of communication with the reactor core during its operation. Thus it aids fast and safe transportation of individual samples in and out of the reactor core with the aid of compressed air. The sample vials are placed inside a polyethylene holder called “rabbit”. The rabbit is then sent to travel through polyethylene tubing between the receiver in the processing hood and the terminus in the reactor core. A blower assembly, moving compressed air through the system, moves and pulls the rabbit between the receiver and the terminus (Shiraki and Liu, 2007)

3.1.3 Gamma-ray counting equipment

In this work, a high purity Germanium (HPGe) Gamma ray spectrometers was used. The spectrometer consists of a Ge detector, a preamplifier, a high-voltage power supply, a spectroscopy linear amplifier and a multichannel analyzer (MCA built in a Personal Computer Analyzer device (PCA) as shown in Fig. 3.2. The characteristics of the high purity Germanium are presented in table 3.1.

Table 3.1; Characteristics of a GEM-70-S HPGe Coaxial Detector (ORTEC)

Type	**GEM-70-S HPGe Coaxial Detector (ORTEC)**
Resolution	1.95keV at 1.33MeV, ^{60}Co
Relative Efficiency	70%
Peak Shape(FWTM/FWHM)	1.83
Peak Shape(FWFM/FWHM)	2.4
Polarity	Positive

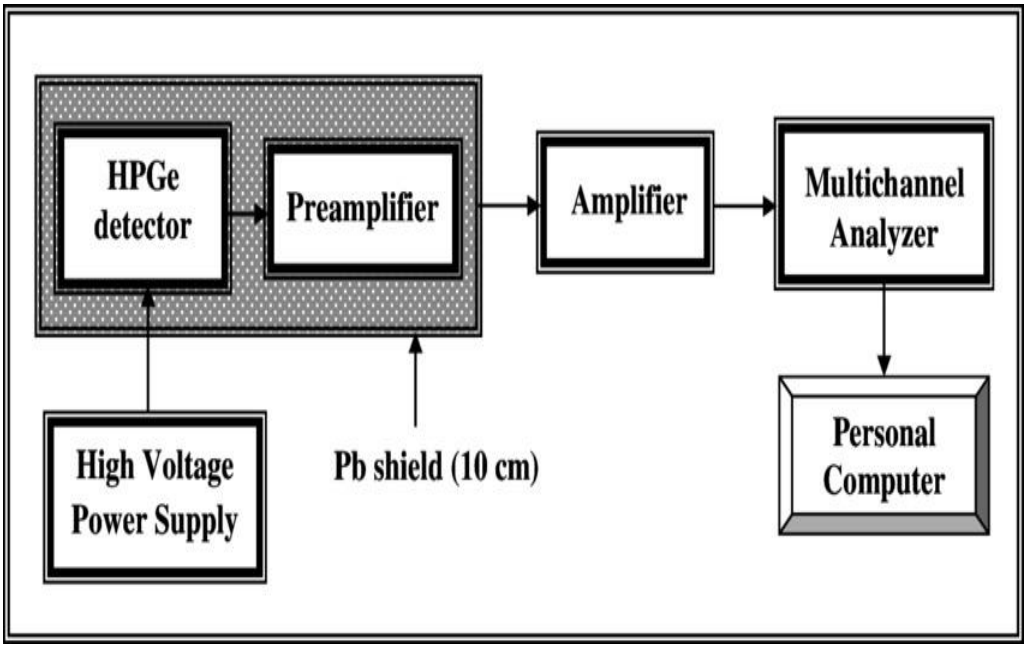


Figure 3.2: The Electronics Block Diagram of HPGe Gamma – Ray Spectrometer.



Plate I: HpGE Detector Set-up

3.1.4 Activation Foils

In this study, three foils were selected according to their availability, nuclear data and their cross-section spectrum. The selected foils are:

- Aluminum-gold (0.134% gold) foil,
- 99.95% Zinc foil,
- 99.8% Zirconium foil

These elements have cross sections and resonance energies with Q_0 values ranging from low to very high and thus serve a quality control of the irradiation facility. The physical characteristics of the thin foils used as flux monitors are presented in Table 3.2 and Table 3.3 summarizes all of the foils used, the neutron interactions of interest, and the useful energy ranges of each interaction. All target isotopes of interest exhibit $\sigma(v) \sim 1/v$ characteristics at energies up to 2-3 eV.

Table 3.2. Physical characteristics of foils used for neutron spectrum monitoring

Element	Material description	Diameter (cm)	Range of mass (mg)
Au	Al-0.1%Au foil; 0.1 mm thick, IRRM-530	0.8	12 - 14
Zn	99.95% Zn foil; 0.025 mm thick, Goodfellow	0.8	4 - 5
Zr	99.8% Zr foil; 0.125 mm thick, Goodfellow	0.8	44 - 46

Table 3.3: Nuclear data for the used foils (Decorte and Simonitis, 2003)

Foil	Target isotope	Product Nuclide	Half life	E_γ (eV)	E_r (eV)	Q_0	Abundance
Al-0.1Au	^{197}Au	^{198}Au	232848	411.8	5.65	15.7	0.955
Zr	^{94}Zr	^{95}Zr	5531328	724.2	6260	5.31	0.4415
				756.73			0.545
	^{96}Zr	^{98}Zr	60264	734.3	338	251.6	97.9
Zn	^{64}Zn	^{65}Zn	21107520	115.5	2560	1.908	0.507
	^{68}Zn	^{69m}Zn	49536	438.6	590	3.19	0.948

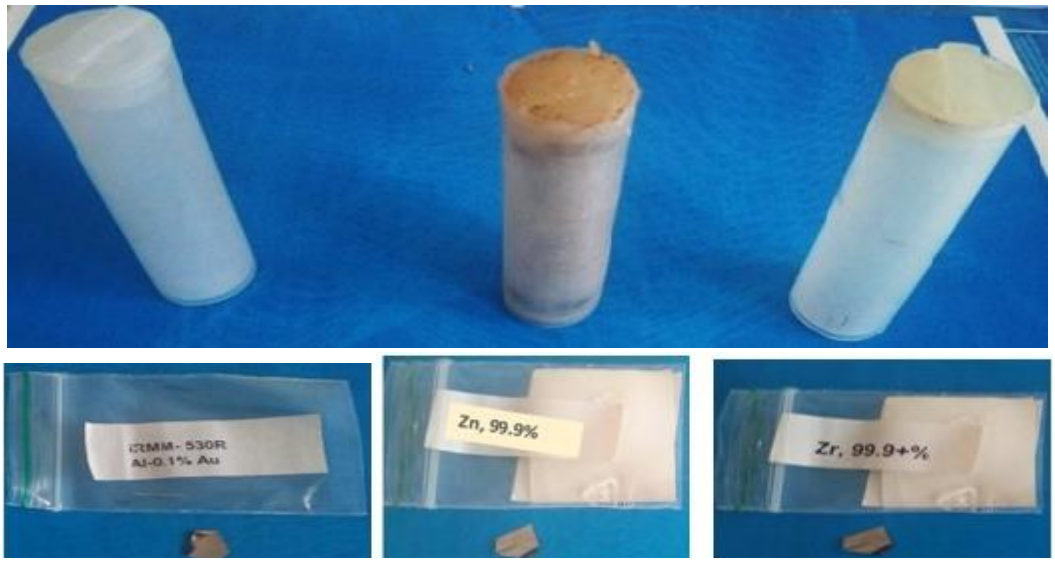


Plate. 2: Set of monitors irradiated in bare condition and with 1mm cadmium cover in Polystyrene vials

3.2 Methodology

3.2.1 Foil Irradiations

The foils were carefully weighed using the same electronic micro balance and on the same day in order to eliminate the systematic error due to weighing of small masses. Two set of the three monitors were prepared and packed in a standard polyethylene vial. One set was irradiated bare and another for irradiation under a cadmium cover of 1 mm thickness. All foils were irradiated at a thermal power level of 15.5 kW, which corresponds to a preset neutron flux value of $5.0\times10^{11} ncm^{-2}s^{-1}$ on the control computer. Irradiation times varied in accordance to the neutron flux in the irradiation sites. The inner irradiation sites had short irradiation times due to high neutron fluxes, while the outer irradiation site had longer irradiation times due to lower neutron fluxes. The irradiation times for the inner irradiation sites is thirty minute (30mins) for the bare foils and one hour (60mins) for the Cd covered foils, while for the outer irradiation sites, the irradiation times are one hour (60mins) and two hours (120mins) for the bare and Cd covered foils respectively with the aim of having comparable activities and similar counting times.

3.2.2 Foil counting/Gamma- ray spectrometry measurement

The activities of ^{198}Au (412 keV, 2.7 days Half-life) was measured four days after irradiation. Two weeks after irradiation, the activity of ^{95}Zr, (724 and 757 keV, half-life 64 days,) was measured. 60 days after irradiation the activity of ^{95}Zn (1115.5 keV, and 244 days half-life) was measured.

The counting times for Al-0.1%Au and 99.8% Zr foils was one hour (1hrs) for both irradiation sites. While the 99.8% Zn foil irradiated at the inner irradiation site was counted for eight hours (8hrs) and that irradiated at the outer site was counted for ten hours (10hrs). After each count has been obtained with the HPGe detector, the collected spectrum was transferred from the MCA to a personal computer (PC) for data analysis

using MAESTRO emulation software. No efficiency calibration was necessary since only the ratio of the bare to the cadmium covered activity is required.

3.2.3 Determination of specific activity

The gamma ray emissions in the collected spectra obtained after a bare and a Cd covered-foil irradiation were used to determined specific activities with the help of the following relationship:

$$A_{sp,} = \frac{N_p / t_m}{(SDC)} \frac{1}{w} \tag{3.1}$$

where A_{sp} and N_p denotes the specific activity and net peak counts, while all other terms have been previously defined.

3.3.4 Determination of the cadmium ratio

Cadmium ratio is defined by the ratio of specific activities obtained after a bare irradiation to that obtained with Cd covered foil irradiation, respectively and is given by:

$$R_{Cd} = \frac{A_{sp,bare}}{A_{sp,cd} / F_{cd}} \tag{3.2}$$

where $A_{sp,bare}$ and $A_{sp,Cd}$ are specific activities obtained after a bare and Cd covered foil irradiation, respectively. The term F_{Cd} is cadmium filter epithermal neutron transmission factor which accounts for absorbed epithermal neutrons by the cadmium cover. This neutron absorption process results in a reduction of the sample's activity. In general, the factor F_{Cd} is mostly ≤ 1 for most elements (De corte, 1987; El Nimr *et al*., 1981; Yu¨cel *et al.* 2004).

3.2.5 Determination of reactor neutron spectrum parameters

The experimental method for the determination of the neutron flux parameters can be classified into three groups based on Cd-ratio method, Cd-covered method and Bare triple-monitor method respectively each involving a set of activation monitors with suited characteristics (De Corte *et. al*., 1981, Decorte, 1987; Dung and Cho, 2003; Ahmed, 2004). Among the various experimental methods available for determining the epithermal deviation factor, the cadmium ratio method is known to yield the most accurate results (De Corte *et. al*., 1981, Decorte, 1987; Dung et.al 2003; Ahmed, 2004; Yavar *et al.*, 2011).

Since NIRR-1 is known to exhibit stable neutron flux characteristics, the parameters '*f*' and α were simultaneously determined using the cadmium ratio method in this work. The Cadmium ratio (multi monitor or dual monitor) method is used when the neutron flux characteristics are known to be stable as a function of time. A set of monitors is irradiated with and without Cd-cover, and the induced activities are measured with a HPGe detector.

3.3.3.1 Cadmium ratio for multi-monitor method

This method is used when the neutron flux characteristics are known to be stable as a function of time. A set of Au, Zn and Zr foils were irradiated with and without cd-cover, and their induced activities were measured with a HPGe detector. The parameter α was obtained as the slope (-α) of the straight line plot of equation (3.15):

$$\log \frac{(\bar{E}_{r,i})^{-\alpha}}{(F_{Cd,i} \cdot R_{Cd,i} - 1) \cdot Q_{0,i}(\alpha) \cdot G_{e,i} / G_{th,i}} \text{ Versus } \log \bar{E}_{r,i} \qquad (3.15)$$

where "*i*" is a monitor with well-known Q_0 value, and $G_{ep,i}$ and $G_{th,i}$ are thermal and epithermal neutron self-shielding correction factors, respectively.

The parameter *f* was obtained from the ordinate value which is equal to log*(1/f)* at $\log \bar{E}_r = 0$ after plotting equation 3.15 .

where flux ratio *f* is defined as:

$$f = (F_{Cd,i} \cdot R_{Cd,i} - 1) \cdot Q_{0,i}(\alpha) \cdot \frac{G_{e,i}}{G_{th,i}} \tag{3.16}$$

Mathematically, by using an iterative procedure for the same number of monitors, Equation. 3.15 can then be written as given below in Equation.3.17, and α value can be found as the root of the equation:

$$\alpha + \frac{\sum_{i=1}^{N}\left[\left\{\log \bar{E}_{r,i} - \frac{\sum_{i=1}^{N}\log \bar{E}_{r,i}}{N}\right\}\left\{\log \frac{(\bar{E}_{r,i})^{-\alpha}}{(F_{Cd,i} \cdot R_{Cd,i} - 1) \cdot Q_{0,i}(\alpha) \cdot G_{e,i}/G_{th,i}} - \frac{\sum_{i=1}^{N}\log \frac{(\bar{E}_{r,i})^{-\alpha}}{(F_{Cd,i} \cdot R_{Cd,i} - 1) \cdot Q_{0,i}(\alpha) \cdot G_{e,i}/G_{th,i}}}{N}\right\}\right]}{\sum_{i=1}^{N}\left\{\log \bar{E}_{r,i} - \frac{\sum_{i=1}^{N}\log \bar{E}_{r,i}}{N}\right\}^2} = 0 \tag{3.17}$$

But in this work, the neutron flux parameter made use of equation 3.15 in the determination of the neutron flux parameters.

3.3.3.1 Cadmium ratio dual-monitor method

The modified Ryves two detector method assumes that when two monitors irradiation site at the same time under the same condition with and without Cd cover alternately, the flux ratio of the two foils f_1 and f_2 are equal under experimental conditions. i.e. (De corte *et.al*, 1979, 2010, Yu¨cel *et. al*, 2004, Tran Van Hung *et. al*, 2004):

$$f_1 \approx f_2 \tag{3.17}$$

where *f* is defined in equation 3.16. This transforms equation 3.18 to:

$$\frac{(F_{Cd,1} \cdot R_{Cd,1} - 1)}{(F_{Cd,2} \cdot R_{Cd,2} - 1)} \approx \frac{Q_{0,2}(\alpha) \cdot \frac{G_{e,2}}{G_{th,2}}}{Q_{0,2}(\alpha) \cdot \frac{G_{e,1}}{G_{th,1}}} \tag{3.18}$$

Substituting equation 2.27b in equation 3.18 and rearranging, then we have:

$$\frac{(F_{Cd,1}\cdot R_{Cd,1}-1)}{(F_{Cd,2}\cdot R_{Cd,2}-1)}-\frac{\left[\dfrac{Q_{0,2}-0.429}{(\bar{E}_{r,2})^{\alpha}}+\dfrac{0.429}{(2\alpha+1)E_{cd}^{\alpha}}\right]\dfrac{G_{e,2}}{G_{th,2}}}{\left[\dfrac{Q_{0,1}-0.429}{(\bar{E}_{r,1})^{\alpha}}+\dfrac{0.429}{(2\alpha+1)E_{cd}^{\alpha}}\right]\dfrac{G_{e,1}}{G_{th,1}}}\approx 0 \qquad (3.19)$$

with this assumption, the f and α values in channels B2 and B4 were obtained from ^{197}Au-^{94}Zr and couple solving equation (3.19) by an iterative procedure using Microsoft-EXCEL Spreadsheet

CHAPTER FOUR

RESULTS AND DISCUSION

4.1 Preamble

The nuclear reactions ^{197}Au(n,γ)^{198}Au, ^{64}Zn(n,γ)^{65}Zn, ^{94}Zr(n,γ)^{95}Zr, were used in the determination of the of the α parameters in order to account for the $1/E^{1+\alpha}$ spectrum. For all experiments, all the nuclear data were taken from the compilation of De Corte (2003), which are summarized in Table 4.1. The thermal and epithermal neutron self-shielding corrections for ^{197}Au(n,γ)^{198}Au and ^{64}Zn(n,γ)^{65}Zn , where neglected and considered as $G_{th} = G_{ep} \cong 1$, while for ^{94}Zr(n,γ)^{95}Zr, $G_{th} = 1$ and $G_{ep} = 0.983$.

Table.4.1: Nuclear data

Foil	Target isotope	Product Nuclide	Half life	E_γ (eV)	$\bar{E}_r$(eV)	Q_0	Abundance
Al-0.1%Au	^{197}Au	^{198}Au	232848	411.8	5.65	15.7	0.955
Zr	^{94}Zr	^{95}Zr	5531328	724.2 756.73	6260	5.31	0.4415 0.545
	^{96}Zr	^{98}Zr	60264	734.3	338	251.6	97.9
Zn	^{64}Zn	^{65}Zn	21107520	115.5	2560	1.908	0.507
	^{68}Zn	^{69m}Zn	49536	438.6	590	3.19	0.948

From the specific activities calculated using Equation 3.1 with the aid of the nuclear data in Table 4.1 and the net peak counts (N_p) from the irradiated foils, the cadmium ratio for each monitor was calculated using Equation 3.2 and presented in Table 4.2.

Table.4.2: Cadmium ratios for Channels B_2 and B_4

Target isotope	**Product Nuclide**	**Experimentally Determined R_{Cd} values**	
		Channel B_2	*Channel B_4*
^{197}**Au**	^{198}Au	2.064 ± 0.004	4.143 ± 0.001
^{94}**Zr**	^{95}Zr	3.396 ± 0.122	11.846 ± 0.633
^{64}**Zn**	^{65}Zn	7.529 ± 0.084	33.6227 ± 0.445

4.2 Results of neutron spectrum parameter in Channel B_2

Results of R_{cd} for each monitor presented in Table 4.1 was determined from the ratio of specific activities, A_{sp} of the bare and Cd covered irradiated the foils. Using these R_{Cd} values, the experimental f and α values in channel B_2 was obtained using the Cd ratio dual monitor from ^{197}Au-^{94}Zr monitor couple by solving equation (3.19) by an iterative procedure based on MS-EXCEL Spreadsheet. As shown in figure 4.1.

A	B	C	D	E	F	G	H	I	J	K	L	M	N
increnent	α	$Q_{0,AU}(\alpha)$	$Q_{0,In}(\alpha)$	$R_{cd,AU}$	$R_{cd,In}$	$E_{r,AU}$	$E_{r,In}$	$Q_{0,AU}$	$Q_{0,In}$	Ecd	$f_{1,Au}$	$f_{2,In}$	f_1-f_2
0.0001	-0.40000000	32.21596913	35.82882783	2.0645	7.77342	5.65	2560.0	15.7	1.908	0.55	33.69531032	246.88080335	-213.18549303
	-0.39990000	32.20909710	35.80045982								33.68812273	246.68533174	-212.99720900
	-0.39980000	32.20222916	35.77211598								33.68093942	246.49002674	-212.80908732
	-0.39970000	32.19536530	35.74379630								33.67376037	246.29488820	-212.62112782
	-0.39960000	32.18850550	35.71550075								33.66658558	246.09991592	-212.43333034
	-0.39950000	32.18164977	35.68722930								33.65941503	245.90510973	-212.24569469
	-0.39940000	32.17479808	35.65898193								33.65224872	245.71046945	-212.05822073
	-0.39930000	32.16795044	35.63075862								33.64508664	245.51599490	-211.87090827
	-0.39920000	32.16110682	35.60255933								33.63792876	245.32168591	-211.68375715
	-0.39910000	32.15426722	35.57438404								33.63077510	245.12754231	-211.49676721
	:	:	:								:	:	:
	-0.04610000	16.99977822	2.58339961								17.78039954	17.80107832	-0.02067878
	-0.04600000	16.99684052	2.58165987								17.77732694	17.78909054	-0.01176361
	-0.04590000	16.99390335	2.57992147								17.77425489	17.77711201	-0.00285712
	-0.04580000	16.99096670	2.57818441								17.77118340	17.76514271	0.00604069
	-0.04570000	16.98803059	2.57644870								17.76811246	17.75318263	0.01492983
	-0.04560000	16.98509501	2.57471432								17.76504208	17.74123178	0.02381030

Au-Zr 1 | Au-Zn1a | AU-ZR1a | Sheet1 | Au-Zr 2 | Au-Zn 1. | Sheet3 | Sheet5 | Sheet2

Determination of f and α from Zr and Au monitor set

$$f = (F_{cd,i} \cdot R_{cd,i} - 1) \cdot Q_{0,i}(\alpha) \cdot \frac{G_{e,i}}{G_{th,i}}$$

f1 = 17.7712 Au

f2 = 17.7651 Zr

α = -0.4580

Figure.4.1:Excel spread sheet indicating the iteration performed to determine the neutron flux parameters (f and α)for Channel B_2 based on cadmium ratio dual monitor method.

Also, the neutron flux parameters were determined using the Cd ratio multi monitor method from the plot of equation (3.15) as shown in figure. 4.2.

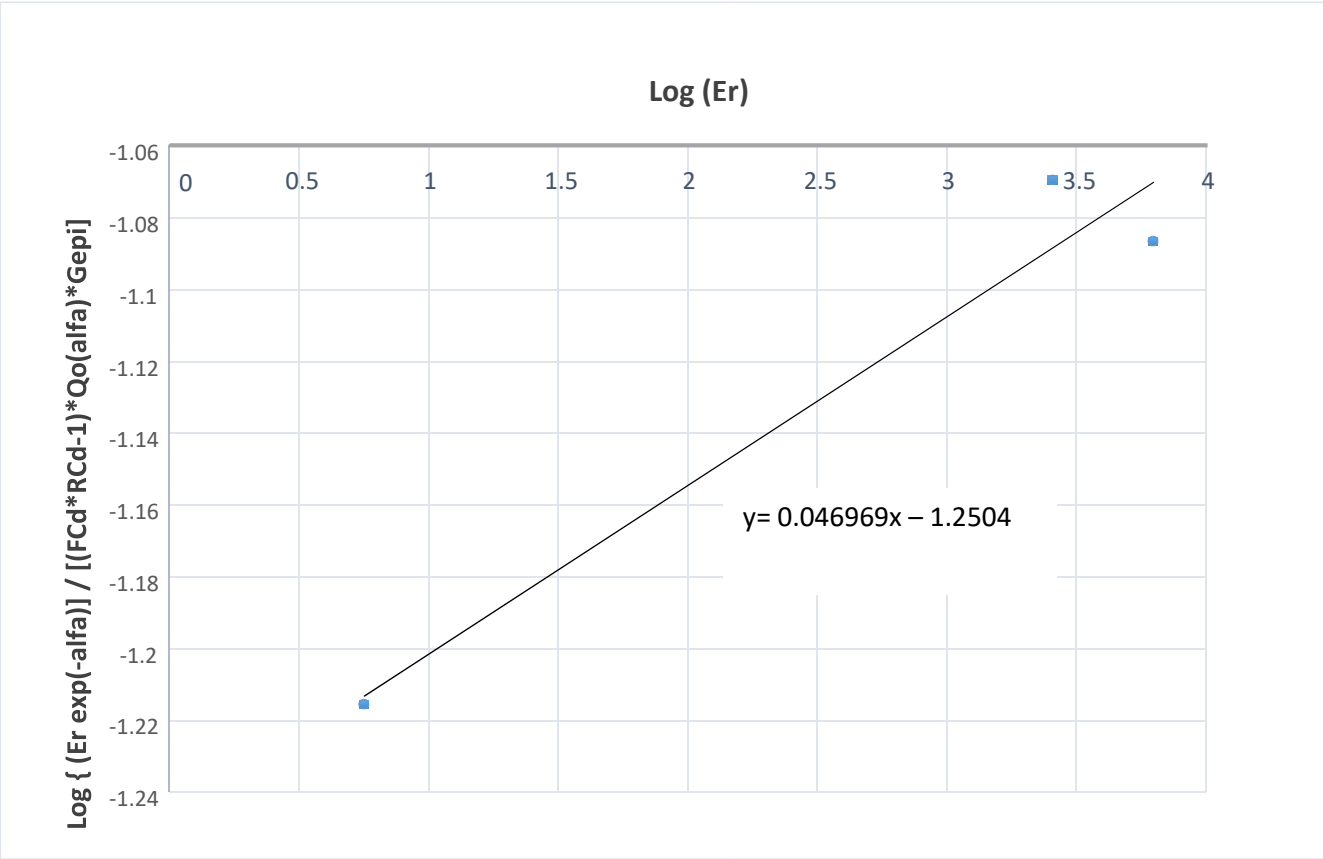


Figure. 4.2: Cd Ratio multi monitor method Channel B2 NIRR-1

4.3 Results of neutron spectrum parameter in Channel B_4

Using thesame R_{cd} results in Table 4.1, the experimental f and α values in channel B_4 was obtained using the Cd ratio dual monitor from ^{197}Au-^{94}Zr monitor couple by solving equation (3.19) by an iterative procedure based on MS-EXCEL Spreadsheet. As shown in figure 4.3.

A	B	C	D	E	F	G	H	I	J	K	L	M	N
increnent	α	$Q_{0AU}(\alpha)$	$Q_{0Zr}(\alpha)$	$R_{cd,AU}$	$R_{cd,Zr}$	$E_{r,AU}$	$E_{r,Zr}$	Q_{0AU}	Q_{0Zr}	Ecd	$f_{1,Au}$	$f_{2,Zr}$	f_1-f_2
0.00010000	-0.40000000	32.21578101	162.80454082	4.14300	11.846000	5.650000	6260.000000	15.70000	5.310000	0.5500	101.25419970	1765.77804974	-1664.52385003
	-0.39990000	32.20890916	162.66216979								101.23260148	1764.23389355	-1663.00129207
	-0.39980000	32.20204139	162.51992495								101.21101609	1762.69110603	-1661.48008994
	-0.39970000	32.19517771	162.37780619								101.18944353	1761.14968592	-1659.96024239
	-0.39960000	32.18831809	162.23581338								101.16788375	1759.60963194	-1658.44174819
	-0.39950000	32.18146253	162.09394642								101.14633672	1758.07094284	-1656.92460611
	-0.39940000	32.17461102	161.95220518								101.12480242	1756.53361733	-1655.40881491
	-0.39930000	32.16776354	161.81058954								101.10328082	1754.99765417	-1653.89437335
	-0.39920000	32.16092010	161.66909940								101.08177188	1753.46305209	-1652.38128021
	⋮	⋮	⋮								⋮	⋮	⋮
	⋮	⋮	⋮								⋮	⋮	⋮
	⋮	⋮	⋮								⋮	⋮	⋮
	0.02390000	15.06716066	4.37596350								47.35608597	47.46170014	-0.10561417
	0.02400000	15.06456925	4.37244818								47.34794117	47.42357294	-0.07563178
	0.02410000	15.06197831	4.36893590								47.33979781	47.38547879	-0.04568097
	0.02420000	15.05938782	4.36542667								47.33165591	47.34741764	-0.01576173
	0.02430000	15.05679779	4.36192048								47.32351546	47.30938948	0.01412598
	0.02440000	15.05420823	4.35841732								47.31537646	47.27139427	0.04398218
	0.02450000	15.05161912	4.35491720								47.30723890	47.23343199	0.07380691

Au-Zn 2 | Sheet1 | Au-Zr 2 | Au-Zn 1. | AU-ZR1a | Sheet3 | Sheet5 | Sheet2 | Sheet4

Determination of f and α from Zr and Au monitor set

$$f = (F_{cd,i} \cdot R_{cd,i} - 1) \cdot Q_{0,i}(\alpha) \cdot \frac{G_{a,i}}{G_{th,i}}$$

f1 = 47.3235 Au

f2 = 47.3094 Zr

α = 0.2430

Figure.4.3:Excel spread sheet indicating the iteration performed to determine the neutron flux parameters (f and α) for Channel B_4 based on cadmium-ratio dual monitor method.

Also, the neutron flux parameters were determined using the Cd ratio multi monitor method from the plot of equation (3.15) as shown in figure 4.4.

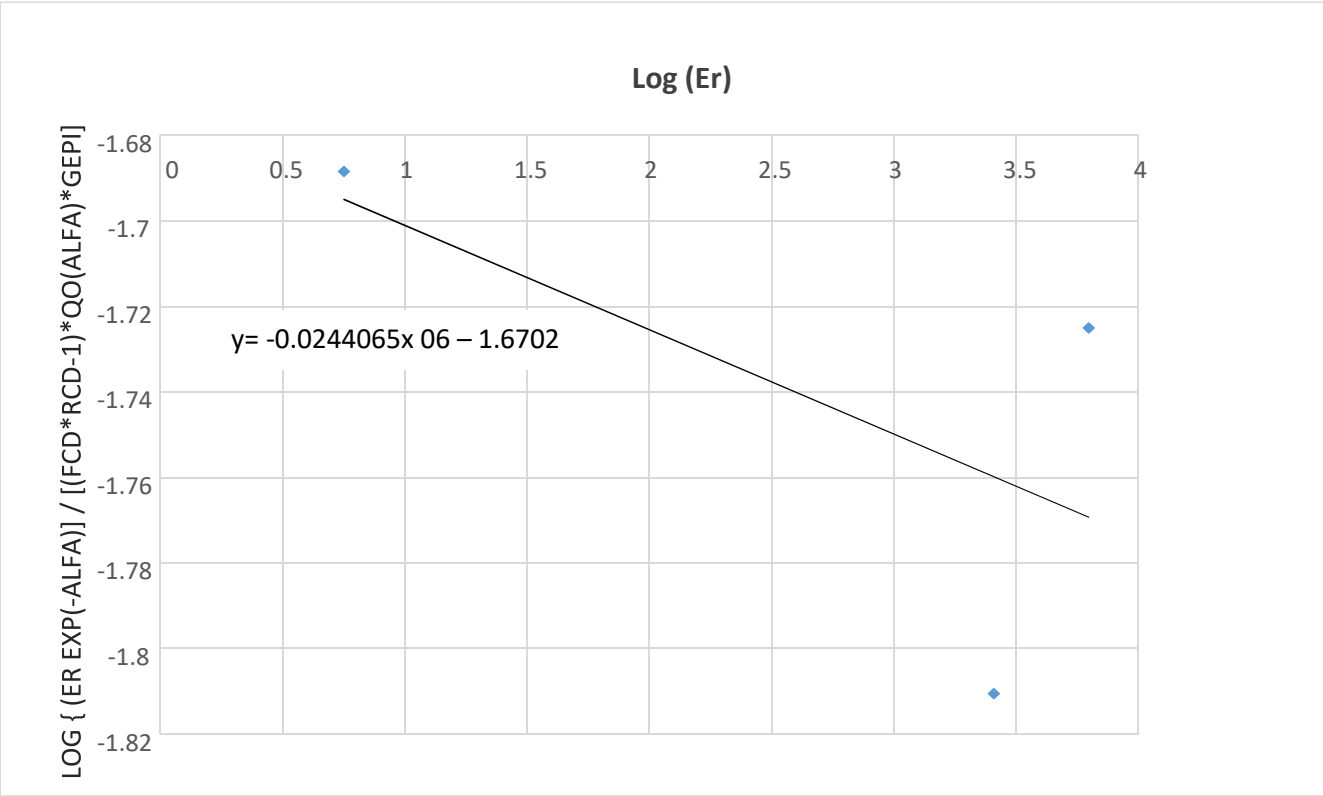


Figure. 4.4: Cd Ratio Multi Monitor Method Channel B4 NIRR-1

The neutron flux parameters obtained for channels B_2 and B_4 using the Cd ratio dual monito method and the Cd ratio multimonitor method are summarized in table 4.2

Table 4.2: Summary of neutron flux parameters obtained using Cd ratio method

Channel	**Dual monitor method**		**Mulitmonitor method**	
	f	α	f	α
B2	17.8 ± 0.3	-0.047 ± 0.0008	17.77 ± 0.34	-0.0458 ± 0.0007
B4	46.8 ± 1.1	0.024 ± 0.0006	47.32 ± 1.36	0.0243 ± 0.0009

The experimental alpha values in channels B_2 and B_4 obtained from the dual and multimonitor methods are good agreement with each other. Negative alpha values in the irradiation channels as already mentioned, correspond to a hardened epithermal spectrum (poorly thermalized) due to the reactor configuration.

When the values of f and α obtained for channels B_2 and B_4 in this work is compared with the value obtained in 2004 after the reactor was commissioned as shown in table 4.3,

Table 4.3: *f* and α values for channels B_2 and B_4 of NIRR-1 determined after commissioning in 2004 compared with this work.

Year/Channels	**Inner Channel**		**Outer Channel**	
	f	α	f	α
2005 (B2 and B4)	19.2 ± 0.5	-0.052 ± 0.002	48.3 ± 3.3	0.029 ± 0.003
This Work (B2 and B4)	17.82 ± 0.3	-0.047 ± 0.008	46.8 ± 1.1	0.024 ± 0.006

It is clearly observed that within the limit of uncertainty, the results as reported agreed very well with each other but the notable fact is the reduction in the flux. In channel B_4 the flux ratio f, decreases from 48.3 to 46.3 with a decrease of 3.11% and the the epithermal shaping factor α decreases from 0.029 to 0.024 with a change of 17.24%. On the other hand, in channel B_2 decreases from 19.2 to 17.8 with a decrease of 7.29% while the epithermal shaping factor α decreases by 9.62% from -0.052 to -0.047 . This variation

compared to earlier works may be attributed to the depletion of the core with time and major modifications modifications carried out. However, it should be highlighted that the physical state of the reactor may have not been exclusively the cause of this variation in the parameters but may have been partly affected by some experimental conditions (such as the mass and geometry of the cadmium plate used).

When the neutron flux parameters obtained in this work for NIRR-1 compared with previous results obtained in NIRR-1 and data for GHARR-1 in comparison with the data for the prototype MNSR as shown in table 4.4, it can be seen that the result obtained in this work shows a level of acceptable of consistency with the previous results from earlier reports.

Table 4.4. Flux parameters obtained in this work for NIRR-1 compared with previous results obtained in NIRR-1 and data for GHARR-1 in comparison with data for the prototype MNSR and other similar facilities

Reactor Facility (Channels)	**Inner Channel**		**Outer Channel**		**Reference**
	f	α	f	α	
MNSR GHARR-1, Accra, Ghana (1 and 6)	18.8	-0.104	49	0.0261	Akaho *et al.*, (2002)
Prototype MNSR Beijing, China	19.8	-0.009	58.5	0.023	Kennedy *et al.*, (2003)
SLOWPOKE-2, DUSR Halifax Canada	18.8	-0.0425	57.1	-0.0098	Kennedy *et al.*, (2003)
SLOWPOKE-2 , Ecole Polytecnic Monreal Canada	19.8	-0.052	55.4	-0.006	Kennedy *et al.*, (2003)
MNSR NIRR-1, Zaria, Nigeria (B4 and B2)	19.2	-0.052	18.3	0.029	Jonah *et al.*, (2005)
MNSR GHARR-1, Accra, Ghana (5 and 7)	17.28	-0.107	40.38	-0.173	Ahmed *et al.*, (2006)
MNSR NIRR-1, Zaria, Nigeria (A1 and A2)	18.4	-0.046	49.5	0.024	Sadiq *et al.*, (2010)
MNSR GHARR-1, Accra, Ghana (5 and 7)	18.34	-0.0479			Baidoo *et al.*, (2013)
MNSR NIRR-1, Zaria, Nigeria (B4 and B2)	17.82	-0.0469	46.79	0.0244	***This Work***

CHAPTER FIVE

SUMMARY

5.1 Conclusion

In summation, this study has characterized the neutron spectra in channels B_2 and B_4 of Nigeria Research Reactor -1 (NIRR-1). The thermal to epithermal flux ratio f of (NIRR-1) were measured and found to be 17.28 for the inner channel B_2 and 46.79 for the outer channel B_4 while the epithermal flux-shaping factor α for these channels were obtained as –0.0469 and 0.0244 respectively. The channels characterized were intentionally selected to compare the present neutron flux parameters with those obtained at the commissioning of the reactor. The result shows good agreement with previous ones determined by Jonah *et al.* 2005 for B_2 and B_4 commissioning of the reactor and those obtained for channels A_1 and A_2 by Sadiq *et al.* in 2010.

It can be categorically stated that, even though the core of NIRR-1 had been critical for over a decade, it is still an excellent source of neutrons for reactor neutron activation analysis if regular configuration changes in the core are made. This result will help to better predict interactions of neutrons with materials both in and around the reactor core and to provide a baseline data for the development of protocols for the use of NIRR-1 for NAA after conversion from HEU to LEU.

5.2 Recommendation

Future work could include carrying out these parameter measurements using neutron transport code (ATTILLA, MCNP, STAY'SL etc.) lt. The neutron activation data should be verified frequently so as to ascertain the status of the neutron flux parameters. This work should be carried out after conversion.

REFERENCES

Acharya, R. and Chatt, A.(2003), Characterization of the Dalhousie University SLOWPOKE-2 Reactor for k_0 -*NAA* and the Application to Medium Lived Nuclides, *Journal of Radioanalytical and Nuclear Chemistry*,257(1):525-529.

Ahmed Y. A, (2013); Parameter measurement, efficiency calibration and quality assurance for a vertical GEM-30195 coaxial HPGe detector, *Nigerian Journal of Physics Vol. 24 June 2013.*

Ahmed Y.A, (2004) Characterization of Irradiation Channels of the GHARR-1 Minature Neutron Source Reactor. *MSc. Thesis, Ahmadu Bello University Zaria.*

Akaho E.H.K. and B.J.B. Nyarko, (2002); Characterization of neutron flux spectra in irradiation sites of MNSR reactor using the Westcott-formalism for the k0 neutron activation analysis method *Applied Radiation and Isotopes 57 (2002) 265–273.*

Alafasi and Chung (1995); Prompt gamma neutron activation analysis, *CRC Press Boca Raton London Tokyo ISBN 0-8493-5149-9.*

Alnour I. A., (2013); Determination of Neutron Flux Parameters in PUSPATI TRIGA Mark II Research Reactor, Malaysia, *J Radioanal Nucl Chem, (2013)296:1231–1237 DOI;10.1007/s10967-012-2375-9.*

Ashbaker .E, (2005); Characterizing the Neutron Spectra in Various Irradiation Facilities within the Oregon State University TRIGA Reactor. *Master's Thesis, Oregon State University.*

Bowen .H.J.M and Gibbons .D, (1963); Radioactivation Analysis, Wantage Research Laboratory Atomic Energy Research Establishment Oxford, *Clarendon Press.*

David Hamilton *; European Commission Institute for Transuranium Elements Postfach 2340, 76125 Karlsruhe, Germany.*

De Corte, F., Moens, L., Simonits, A., De Wispelaere, A., and Hoste, J.(1979a), Instantaneous α-Determination in the $1/E^{1+\alpha}$ Epithermal Neutron Spectrum, *Journal of Radioanalytical and Nuclear Chemistry, 52(2): 295-304.*

De Corte, F., Sordo-El Hammami, K., Moens, L., Simonits, A. and Hoste, J.(1979b), Modification and Generalization of Some Methods To Improve The Accuracy Of α-Determination in the $1/E^{1+\alpha}$ Epithermal Neutron Spectrum, *Journal of Radioanalytical Chemistry, Vol. 52, No. 2 (I 979) 305-316.*

De Corte, F., Sordo-El Hammami, K., Moens, L., Simonits, A., De Wispelaere, A. and Hoste, J.(1981): The Accuracy and Precision of The Experimental α-Determination in the Epithermal Reactor-Neutron Spectrum. *Journal of Radioanalytical Chemistry, VoL 62, No. 1-2 (1981) 209-255.*

De Corte. F, (1987); The k_0-Standardization Method: A Move to the Optimization of Reactor Neutron Activation Analysis, Habil. Thesis, *University of Gent.*

De Wispelaere A. et al, (2006); Re-determination and re-evaluation of the f and α parameters in channels Y4 and S84 of the BR1 reactor, for use in k0-NAA at DSM Research, *Nuclear Instruments and Methods in Physics Research A 564 (2006) 636–640*

Di Tigliole A.B, Cammi .A, D. Chiesa, Manera .S, M. Nastasi, L. Pattavina, M. Sisti (2014); TRIGA Absolute Neutron Flux Measurement Using Activated Isotopes, Progress in nuclear energy 70(2014) 249-255, *http://dx.doi.org/10.1016/j.pnucene.2013.10.001*.

DOE, (1993); Department of Energy Fundamentals Handbook**,** Nuclear physics and reactor theory, Volume 1**,** *DOE-HDBK-1019/1-93.*

Dung H.M, (2010); Re-characterization of irradiation facilities for k0-NAA at RPI after conversion to LEU fuel and re-arrangement of core configuration, *Nuclear Instruments and Methods in Physics Research A 622 (2010) 438–442.*

Dung, H.M. and Cho, S.Y. (2003), A simple Method for α Determination, *Journal of Radioanalytical and Nuclear Chemistry, Vol. 257, No. 3 (2003) 573.575.*

Franca .R .S ¸ (2012); Neutron Flux Characterization and Design of UFTR Radiation Beam Port Using Monte Carlo Methods, *Masters Thesis, University Of Florida.*

Freitas M. C. et al (2003); Neutron flux and associated k0 parameters in the RPI after the last configuration change, *Journal of Radioanalytical and Nuclear Chemistry, Vol. 257, No. 3 (2003) 539.543.*

Glascock M. D, (2004); An Overview of Neutron Activation Analysis, *University of Missouri Research Reactor* (MURR), *Research Reactor, University of Missouri, Columbia,MO 65211, retrieved from; https://www.researchgate.net/publication/228643668_An_overview_of_neutron_activation_analysis.*

Greenberg et al, (2011); Neutron activation analysis: A primary method of measurement, *Spectrochimica Acta Part B 66 (2011) 193–241.*

Hainoun .A, Alhabit. F, (2007); Safety Analysis of MNSR Reactor during Reactivity Insertion Accident Using the Validated Code PARET, *International Conference on Research Reactors: Safe Management and Effective Utilization 5–9 November 2007, Sydney, Australia*.

Jonah, S.A., Balogun, G.I., Umar, I.M. and Mayaki, M.C. (2005), Neutron Spectrum Parameters in Irradiation Channels of the Nigerian Research Reactor-1 (NIRR-1) for the k_0 -*NAA* Standardization, *Journal of Radioanalytical and Nuclear Chemistry, 266(1): 83-88.*

Jovanovic, S., Vukotic, P., De Corte, F., Simonits,A., Moens, L. and Hoste, J. (1987); The Effective Resonance Energy as a Parameter in (n, γ) Activation Analysis with Reactor Neutrons, *Journal of Radioanalytical and Nuclear Chemistry*,111(1): 177-185.

Jovanovic. S, De Corte, F., Moens, L., Simonits A., De, Vlahovic. V, Zejnilovic. R, Hoste, J., (1987); Epithermal Neytron Flux Distribution and itsImpact on (n,γ) Activation Analysis Result.*Research Associate of the National Scientific Research, Belgium.*

Kennedy. G., St.-Pierre. J, Wang. K, Zang Y, Preston. J, Grant. C, Vutchkov. M, (2000): Activation constants for SLOWPOKE and MNS reactors calculated from the neutron spectrum and k_0 and Q_0 values; *Journal of Radioanalytical Chemistry, 245 (1) pp 167-172.*

Kubešová, I.M, (2012), k_0 standardization in neutron activation analysis at LVR-15 Reactor in Řež. *PhD Thesis.Brasil.*

Kulage Z.A, (2010); Characterized the neutron flux spectrum at the Missouri University of Science and Technology Research Reactor *MSc. Thesis.*

Lamarsh, (1982); Introduction to Nuclear Engineering, *Third Edition.*

Masood .I, Muhammad .A, Showket P, (2002); Parametric tests and measurements after shimming of a beryllium reflector in a miniature neutron source reactor (MNSR), *Annals of Nuclear Energy 29 (2002) 1609–1624.*

Moens. L., De Corte. F, Simonits .A, De Wispelaere.A, Hoste .J, (1979):The Effective Resonance Energy $\bar{E}_r$ as a Parameter for the Correction of Resonance Integrals in the $1/E^{1+\alpha}$ Epithermal Spectrum Spectra; Tabulation of $\bar{E}_r$ Values for 96 Isotopes, *Journal of Radioanalytical and Nuclear Chemistry*, 52(2): 379-387.

Moteff, (1970); Neutron Fluence Measurements, *IAEA Technical Reports Series No 107 STI/DOC/10/107.*

Mukhin, K.N. (1970). Nuclear Physics; Macdonald Technical and Scientific; London.

Murugeshan and Sivaprasath 2009; Modern Physics *Revised Multicolored Edition, S.Chand and Company Limited ISBN: 81-219-2801-X, Code: 16A333.*

Musa .Y, (2012), Determination of Axial and Radial Neutron Flux Distribution in the Nigeria Research Reactor – 1 (NIRR-1) using foil activation technique. *MSc. Thesis, Ahmadu Bello University Zaria.*

Negoita .C.C, (2004) Measurement of Neutron Flux Spectra in a Tungsten Benchmark by Neutron Foil Activation Method. *PhD Dissertation. Institut für Kern- und Teilchenphysik,Italy.*

Njinga R.L. et al, (2012); Determination of Neutron Flux Parameters after Installation of Cd-Lined for Implementations of ENAA and FNAA with NIRR-1, *International Journal of Applied Science and Technology Vol. 2 No. 1.*

Potts. P. J (1987), A Handbook Of Silicate Rock Analysis. Springer Science Business Media, New York, *ISBN 978-94-015-3988-3 (eBook), DOI 10.1007/978-94-015-3988-3, Pp 399-435.*

Radulović, Vladimir & Trkov, Andrej & Jaćimović, Radojko & Jeraj, Robert. (2014). Measurement of the neutron activation constants Q 0 and k 0 for the 27Al(n, γ)28Al

reaction at the JSI TRIGA Mark II reactor. *Journal of Radioanalytical and Nuclear Chemistry. 298.*

Ryves.T. B, (1969) A New Thermal Neutron Flux Convention, *Metrologia, Vol. 5, No. 4, 1969.*

Sadiq .U, Jonah .S.A, Nasiru .R, and Zakari .Y.I, (2010), Neutron Spectrum Parameters in Two Irradiation Channels of The Nigeria Research Reactor-1 (NIRR-1) for use in k0-NAA, *Bayero Journal of Pure and Applied Sciences, 3(1): 220 – 223.*

Şahin .D, Radulovic. V, Lindstrom .R.M, Trkov. A, (2014): Reevaluation of neutron flux characterization parameters for NIST RT-2 facility, *journal of radioanalytical and nuclear chemistry · march 2014 DOI: 10.1007/s10967-014-3076-3.*

SAR, (2012); Updated Safety Analysis Report of Nigeria Research Reactor-1, Technical Report CERT/NIRR-1/FSAR-01, CERT, ABU, Zaria, Nigeria.

Sheyin .F.T, Oladipo M. O. A., Jonah S. A, Sadiq .U, (2015); Determination of α in the Cadmium Lined Irradiation Channel of the NIRR-1 for Use in *ko*-ENAA, *World Journal of Nuclear Science and Technology, 2015, 5, 233-240 DOI 10.4236/wnst.2015.53023*

Sheyin, F.T, (2015), Characterization of the Cadmium Lined Irradiation Channel of the Nigeria Research Reactor-1 (NIRR-1) and its Application for Elemental Determination in Some Legumes. *PhD. Thesis. Ahmadu Bello University Zaria.*

Shiraki. R and Liu H. B., (2007), Neutron Flux Measurements by Activation Analysis, McClellian Nuclear Radiation Centre.

Shokr, A.M and Abou Yehia (2009), Safety Considerations for Core Management and Fuel Handling for Research Reactors. *Research Reactor Operation & Maintenance Session VI, pp.20-37, European Nuclear Society, ISBN 978-92-95064-07-2.*

Sogbadji R. B. M., Nyarko B. J. B., Akaho E. H. K., Abrefah R. G, (2011); Determination of Neutron Fluxes and Spectrum Shaping Factors in Irradiation Sites of Ghana's Miniature Neutron Source Reactor (MNSR) by Activation Method after Compensation of Loss of Excess Reactivty, *World Journal of Nuclear Science and Technology, 2011, 1, 50-56 doi:10.4236/wjnst.2011.12009.*

Soliman, M.A. M, (2012), Enhancements and Health-Related Studies of Neutron Activation Analysis Technique. *PhD Thesis, Cairo, Egypt.*

Stefaan .P, Frank .H, Piotr ,R, Nestor .E, Gorka .A, (1997); Neutron Activation Analysis with Standardization: General Formalism and Procedure *Nuclear Spectrometry Radiation Protection Department SCK-CEN, BLG-7G0, Studihchntrum Voor Kernenergie Centre De L'energie Nucleaire, ISBN BE9800001.*

Verheijke, M. L., (1992); Instrumental Neutron Activation Analysis Developed for Silicon Integrated Circuit Technology. *PhD. Thesis, Eindhoven*.

Vu. C.D, Thien.T.Q, Doanh, H.V, Quyet .P.D, And Dien T.T.T, N.N, (2014): Characterization of neutron spectrum parameters at irradiation channels for neutron activation analysis after full conversion of the Dalat nuclear research reactor to low enriched uranium fuel, *Nuclear Science and Technology, Vol. 4, No. 1(2014), pp. 70-75.*

Yavar A.R, Sarmani S. B., Khalafi .H, Wood A. K., Khoo .K. S. (2011); Overview of INAA Method and its Application in Malaysia. Journal *Of Nuclear And Related Technologies, Volume 8, No. 2, December, 2011.*

Yücel .H and Karadag. M, (2004); Experimental determination of the α-shape factor in the $1/E^{1+\alpha}$ epithermal-isotopic neutron source-spectrum by dual monitor method, *Annals of Nuclear Energy 31 (2004) 681–695*.